JET PROPULSION LABORATORY

CALIFORNIA INSTITUTE OF TECHNOLOGY

PASADENA, CALIFORNIA

MEMORANDUM #7

CHARACTERIZATION OF RTG PERFORMANCE IN BOTH AIR AND VACUUM

May 20, 1970

Prepared For:
Jet Propulsion Laboratory
Pasadena, California
Contract No. 952808

This work was performed for the Jet Propulsion Laboratory, California Institute of Technology, sponsored by the National Aeronautics and Space Administration under Contract NAS7-100.

by

Dean Leonard
Scott Luebbers
and
Valvo Raag
Resalab Scientific
Menlo Park, California

TABLE OF CONTENTS

LIST OF FIGURES

LIST OF SYMBOLS

A	empirical constant
a	empirical constant
A_C	convective radiator area in cm^2
A_e	effective insulator area in cm^2
	fraction of heat lost to structural members
a_n	n-type couple leg area in cm^2
A_n	total n-type couple leg area in cm^2
a_p	p-type couple leg area in cm^2
A_p	total p-type couple leg area in cm^2
A_R	radiative area in cm^2
b	empirical constant
β	convective power
C	specific heat at constant volume
δ	electrical loss factor = 1.05
ϵ_r	radiator emissivity
F	radiator view factor
γ	exponent
I_S	current/string in amperes
I	load current in amperes
K	Boltzmann constant, 1.38×10^{-16} erg/ ^oK
$k\ (T)$	temperature dependent thermal conductivity in watt/cm ^oK
$\langle k \rangle$	effective thermal conductivity in watt/cm ^oK
$\langle k \rangle_I$	effective insulation thermal conductivity in watt/cm ^oK

k_i insulation thermal conductivity in watt/cm ^{o}K

k_c conductive component of conductivity in watt/cm ^{o}K

k_{con} convective component of conductivity in watt/cm ^{o}K

k_g gas conductivity in watt/cm ^{o}K

k_r radiative component of conductivity in watt/cm ^{o}K

k_v vacuum conductivity in watt/cm ^{o}K

K_T total radial thermal conductivity in watt/cm ^{o}K

K convective heat transfer coefficient in watt/cm ^{o}K

λ radial fraction of heat input

ℓ thermocouple length in cm

L generator axial length in cm

M molecular mass, gm

m load factor = R_L / R_g

μ visiosity, poise

n number of parallel thermocouple branches

N total number of thermocouples

N_S number of series-connected thermocouples

η generator efficiency

η_f fin efficiency

P_o generator power output in watts

q heat flux in watts/cm^2

Q total heat in watts

Q_{in} heat input in watts

Q_c convective heat flow in watts

Q_r radiative heat flow in watts

Q_{rej} heat rejected from radiator in watts

R_i couple internal resistance in ohms

R_g generator internal resistance in ohms

$\rho(T)$ temperature dependent electrical resistivity in Ω-cm

$<\rho>$ average electrical resistivity in Ω-cm

$S(T)$ temperature dependent Seebeck coefficient in $V/^{o}K$

$<S>$ average Seebeck coefficient in $V/^{o}K$

S Sutherland constant, ^{o}K

σ Stefan-Boltzmann constant = 5.67×10^{-12} watts/cm $^{2}{}^{o}K^{4}$

$\bar{\sigma}$ collision diameter cm

T position dependent temperature in ^{o}K

T_{amb} ambient temperature in ^{o}K

T_C cold junction temperature in ^{o}K

T_H hot junction temperature in ^{o}K

T_r radiator temperature in ^{o}K

$\Delta T = T_H - T_C$

$\Delta T_C = T_C - T_r$

V voltage in volts

V_L load voltage in volts

X variable defining flow conditions at RTG surface

Z product of Prandtl and Groshof numbers

I. INTRODUCTION

Radioisotope thermoelectric generators (RTG's) used on unmanned spacecraft for auxiliary onboard electrical power are commonly fueled prior to launch. Unless special provisions are made to modify the environment on the launch pad, this means that prior to and during launch there is a period of time that the RTG's operate in an air environment. The effects of such air operation on RTG performance are basically of two types. First, the air environment temporarily modifies RTG performance from its design vacuum values by changing the external and in an unsealed system also the internal heat transfer characteristics of the RTG. Subsequent vacuum operation is unaffected by these temporary changes in RTG operating environment and the RTG will exhibit its original design performance in an eventual space environment. Second, operating in an air environment may permanently modify the physical characteristics of certain components of the RTG such that design performance values are not recovered in a subsequent vacuum operation. Mechanical strength characteristics of certain RTG components may also be affected. Permanent changes in RTG operating behavior as a result of air exposure are usually associated with irreversible chemical and/or physical processes caused by reactions and interactions with oxygen.

Because oxygen poses a serious problem to RTG's that use lead and tellurium compounds and alloys, it is accepted practice with devices of this type to hermetically seal them. Prior to final sealing, such devices are frequently also back-filled with an inert gas in order to reduce the volatility of the thermoelectric material. The result of this procedure is that neither permanent nor temporary effects usually occur internal to telluride RTG's as a result of air operation. In air, however, the external heat transfer characteristics of the RTG are modified by an enhanced heat rejection rate from the outer surface of the device because radiation heat transfer is supplemented by convection. In air, the RTG consequently operates at hot and cold side temperatures, and thus also a performance level, that are lower than the vacuum design values. In order for this effect to be only temporary, it is necessary to use materials for the RTG casing and radiator, including radiator emittance coating, that are insensitive to oxygen.

The air operation of silicon-germanium RTG's presents a situation somewhat different from that encountered with telluride generators. Unlike lead and tellurium compounds and alloys, silicon-germanium alloys, are not adversely affected by operation in air. This is also true of the most common silicon-germanium thermocouple configuration, the so-called Air-Vac thermocouple, that uses components which in their respective general ranges of operating temperatures are not adversely affected by air, i.e. by oxygen. Inasmuch as volatility is not a problem either with silicon-germanium Air-Vac thermocouples, it may appear that silicon-germanium RTG's designed for operation in space vacuum require neither hermetic sealing nor any other modifications to also permit pre-launch and launch operation in air. Whether this is really true or not depends on the sensitivity to air of silicon-germanium RTG components other than the Air-Vac thermocouples. Because relatively little effort has been expended to date on the design and development of silicon-germanium RTG's, the effects of air operation on RTG performance have never been fully investigated for silicon-germanium systems. Nevertheless, because of their proven relative stability of performance and reliability, it is namely silicon-germanium Air Vac thermocouples that probably will be used in second-generation RTG's intended for use in future extended-life space missions. It is the purpose of the present memorandum therefore to conduct a preliminary investigation of the effects of air operation on silicon-germanium RTG performance. Initially the generator internal components are considered exposed to the air environment. After evaluating generator performance under these conditions, inert gases are introduced into a hermetically sealed generator and the generator performance is re-examined. The gases included in this study are: Argon, Helium, Krypton, and Xenon. In terms of the temporary and permanent effects discussed above, the primary intent of the present study is to consider the former of these in some detail and to point out in a general manner some more important of the possible latter-type effects. Because in some applications power is required from the RTG even during the launch phase, another and related purpose of the present study is to determine the amount of such power available from typical silicon-germanium RTG's in air operation and with various internal gases.

II. HEAT TRANSFER MODEL

The present description of the theoretical aspects of RTG performance in both air and vacuum will primarily consider heat transfer effects. The theoretical model for the thermoelectric conversion process is independent of generator environment and has been throughly discussed previously (see for example References 1 & 2). In vacuum, heat transfer is due only to radiation and conduction; whereas, in air, convective heat transfer must also be included.

This section of the report assumes an idealized generator configuration for purposes of a mathematical model. The generator is considered to have radial symmetry about an enclosed heat source. The ends of the generator are assumed impervious to heat flow (this is equivalent to assuming constant end losses in actual RTG calculations) and the sides consist of thermoelements separated by thermal insulation. The inner and outer surfaces of the side walls are assumed to be such that only radial heat flow occurs within the walls. The hot and cold junction temperatures of the thermoelements depend on the temperatures of the inner and outer surfaces of the walls; the emissivities of the walls are assumed to be uniform.

HEAT TRANSFER TO THE RADIATOR

The total heat transported though the walls of the generator generally consists of heat passing through the thermoelements and shunt heat passing through the thermal insulation that surrounds the thermoelements. The total heat transferred through the walls of the generator is independent of generator environment except for possible modifcation of the thermal conductivity of insulation. In general, the insulation thermal conductivity, k_I, may be separated into two components:

$$k_I = k_c + k_r \qquad (2\text{-}1)$$

Where k_c and k_r represent the conductive and radiative components respectively. Whereas the conductive term dominates in fibrous insulations, it is the radiative term that is usually more important in foil insulations. In general, the two conductivity terms have a different power dependence on temperature. For the case of foil insulation it has been found that the two components of thermal conductivity may be approximated by (Ref. 3):

$$k_c = aT \ , \tag{2-2}$$

$$k_r = bT^3 \ . \tag{2-3}$$

Where a and b are constants and T is the temperature of the foil insulation. For any insulation, however, a power law approximation may be made for the thermal conductivity over limited ranges of temperatures as follows:

$$k_I = c\ T^{\gamma} \tag{2-4}$$

As shown in appendix A, an effective (average) thermal conductivity, $<k_I>$, here applied to the insulation, may be defined as:

$$q_I = <k_I> \frac{\Delta T}{\ell} = k_I\,(T)\ \frac{dT}{dx} \tag{2-5}$$

Where q_I is the heat flux through the insulation, T is temperature, and ℓ and x are length parameters. Integration of Eq. (2-5) yields:

$$<k_I> = \frac{1}{\Delta T} \int_{T_C}^{T_H} k_I\,(T)\,dT. \tag{2-6}$$

Using average thermoelectric properties (see Appendix A), the heat balance at the hot junction of the thermoelements may be written as:

$$Q_{in} = <k_I> A_e \frac{\Delta T}{\ell} + <k_n> A_n \frac{\Delta T}{\ell} + <k_p> A_p \frac{\Delta T}{\ell} + NI_S ST_H \tag{2-7}$$

$$- 1/2\ NI_S^2 R_i \ ,$$

Where Q_{in} is the total heat input, A_e is the total effective area of thermal insulation, ΔT is the temperature difference between the hot and cold junction temperatures, T_H and T_C respectively, ℓ is the thermoelement length, N is the number of thermocouples, I_S is the series current per thermocouple, R_i is the internal electrical resistance of a couple and A_n and A_p are the total cross-sectional areas of the n- and p-type thermoelements respectively. The thermophysical properties of the Seebeck coefficient and thermal conductivity are denoted by S and k respectively. The subscripts n, p and I pertain to n-and p-type thermoelements and the thermal insulation. Note that S is defined by $S=S_p-S_n$.

Equation (2-7) is one of two basic equations required in the establishment of thermoelement hot and cold junction temperatures, and thus of thermoelectric generator performance. The other such equation pertains to heat rejection from the generator and is discussed below for vacuum as well as air operation.

HEAT REJECTION FROM THE RADIATOR IN VACUUM OPERATION

It is assumed that heat rejection from the radiator is strictly radiative in vacuum. The total heat rejected is given by:

$$Q_{rej} = Q_{in}\ (1-\eta) \tag{2-8}$$

where η is the conversion efficiency of the thermoelectric generator. Efficiency enters the above equation because ηQ_{in} of heat is converted to electrical power output. Using the radiation equation, Eq. (2-8) may be rewritten as:

$$Q_{in}\ (1-\eta) = \sigma\, \epsilon_r \eta_f F A_R\ (T_R^4 - T_{amb}^4)\ , \tag{2-9}$$

Where σ is the Stefan-Boltzmann constant, ϵ_r is the radiator emissivity, η_f is the fin effectiveness, F is the view-factor, A_R is the radiator area, T_R is radiator base temperature and T_{amb} is the effective external heat sink temperature.

After allowances are made for a temperature drop due to conducted heat between the radiator base and thermoelement cold junctions, Eqs. (2-7) and (2-9) allow the determination of thermoelement hot and cold junction temperatures in vacuum operation. Because the efficiency which enters Eq. (2-9), depends upon both T_H and T_C, it is necessary to solve Eqs. (2-7) and (2-9) iteratively. The efficiency is initially given a small but arbitrary value to allow a first approximation estimate of T_H and T_C. The generator performance is then calculated and the new efficiency value substituted into equation (2-9). The iteration is continued until the junction temperatures converge to within any desired degree of accuracy.

HEAT REJECTION FROM THE RADIATOR IN AIR OPERATION

In addition to radiative heat rejection from the radiator, convective heat transfer also takes place in the air operation of a thermoelectric generator. For present purposes it is assumed that radiative and convective heat transfer terms are additive. Equation (2-9) will accordingly be rewritten as:

$$Q_{in}(1-\eta) = \sigma\epsilon_r\eta_f F A_R\left[T_R^4 - T_{amb}^4\right] + KA_c\left[T_R - T_{amb}\right]^{\beta} = Q_r + Q_c \,, \qquad (2-10)$$

Where K is the convective heat transfer coefficient, A_c is the total radiator area that contributes to convective heat transfer, β is an exponent, and Q_r and Q_c represent radiative and convective heat transfer respectively. The convective heat transfer coefficient, K, and the exponent, β, depend upon the particular mode of convective heat transfer applicable to a given situation. In the case of natural convection from vertical cylinders, the numerical values of K and β depend upon whether turbulent or laminar heat flow exist in the boundry layer between the radiator surface and the adjacent environment. It can be shown (Ref. 4) that a variable, X, establishes the boundary layer flow conditions in accordance with type of flow as follows:

Laminar range	$10^4 < X \leq 10^9$
Turbulent range	$10^9 \leq X < 10^{12}$

The quantity X may be defined as:

$$X = 6.37 \times 10^{-5} \times L^3 \left(T_R - T_{amb}\right) Z \qquad (2\text{-}11)$$

Where L is the vertical height of generator and Z is the product of the Prandtl and Grashof numbers.

Figure 1 has been reproduced from Reference 4 to permit calculation of the variable Z. The film temperature in Figure 1 is defined as the mean temperature between the ambient and radiator temperatures.

Depending on the type of flow, the convective heat transfer from the radiator may be written as:

$$Q_c = 44.8 \times 10^{-5} \times L^{-1/4} \times A_R \times \left(T_R - T_{amb}\right)^{1.25}, \qquad (2\text{-}12)$$

(Laminar flow)

and

$$Q_c = 29.4 \times 10^{-5} \times A_R \times \left(T_R - T_{amb}\right)^{1.33}. \qquad (2\text{-}13)$$

(Turbulent flow)

Substituting Eqs. (2-12) and (2-13) into Eq. (2-10) yields

$$Q_{in}\,(1-\eta) = \sigma \epsilon_r A_R \left(T_R^4 - T_{amb}^4\right) + 44.8 \times 10^{-5} \times L^{-1/4} \qquad (2\text{-}14)$$

$$\times A_R \left(T_C - T_{amb}\right)^{1.25}, \qquad \text{(Laminar flow)}$$

and

$$Q_{in}\,(1-\eta) = \sigma \epsilon_r A_R \left(T_R^4 - T_{amb}^4\right) + 29.4 \times 10^{-5} \times A_R \qquad (2\text{-}15)$$

$$\left(T_R - T_{amb}\right)^{1.33}. \qquad \text{(Turbulent flow)}$$

where the fin effectiveness and view factor are taken to be unity and the convective and radiative area are considered equal ($A_c = A_R$).

Equations (2-7), (2-14), and (2-15) are the equations necessary to determine the thermoelement hot and cold junction temperatures in air operation. As before, the dependence of Eqs. (2-14) and (2-15) on efficiency again requires an iterative calculation. The non-integral power dependence of temperatures in Eqs. (2-14) and (2-15) introduces an additional complication. The Newton-Ralphson approximation technique may be used to determine T_R. A discussion of this technique may be found in most books on Advanced Calculus.

III. COMPUTATIONAL METHODS

In order to calculate the performance of a thermoelectric generator in air as well as in vacuum, the dimensional parameters of the overall generator and generator components are required as inputs to the model discussed in the preceding section. Thermophysical properties of the thermoelements, thermal insulation and heat rejection system are determined from previously reported data. With this information and the known heat input, the performance of any thermoelectric generator may be established. The only uncertainties which may exist in the performance calculations are those associated with the thermophysical properties of the various materials used and the heat transfer model employed. In the following section, in which actual performance data are compared to performance calculated with the model described in this memorandum, it will be seen that close agreement is obtained between theory and measurement. In cases where performance data exist and precise thermophysical property data are lacking, the described computational methods may be used to back calculate the unknown property data.

HEAT BALANCING

As a starting point in the calculation of thermoelectric generator performance, the heat must be balanced for the system. Since the performance of the power system is governed by heat emanating from the heat source and the resultant temperature gradients, a reasonable estimate of various losses must be made. The heat source is considered to be completely surrounded by either thermoelectric elements, thermal insulation or heat source support members. Although the exact configuration of the generator is not of particular importance, careful consideration of effective areas must be made. Figure 2 depicts a typical cylindrical thermoelectric generator and illustrates some important considerations in the balancing of heat.

Heat flowing from the heat source may be decomposed into radial and axial components. The axial flow is composed of heat conducted through the heat source support structure and that lost through thermal insulation on the ends. These

heat losses serve no useful function in the energy conversion process; quite the contrary, they detract from the heat available to the thermoelements. The radial heat is similarly divided into two components. The first component comprises the heat that passes through the thermoelements, while the other component consists of heat lost through the thermal insulation. Both of these radial heat flow components are considered to consist of simple conduction processes that may be described by means of effective values of thermal conductivity and cross-sectional area. The thermal conductivity values are integrated averages over the appropriate temperature ranges being considered.

To determine the radial heat flux passing through the thermal insulation, an effective insulation area must be used. Since this area is dependent upon radius, the radial heat flux density may be written as:

$$q = \frac{Q}{2\pi r L} = k \frac{dT}{dr} , \tag{3-1}$$

Where Q is the total radial heat flowing through the insulation, r is the radius and L is the axial length of insulation.

Rearrangement and integration of Eq. (3-1) yields:

$$Q \int_{r=a}^{r=b} \frac{dr}{r} = 2\pi L \langle k \rangle \Delta T, \tag{3-2}$$

Or:

$$Q = \frac{2\pi L}{\ell n \frac{b}{a}} \langle k \rangle \Delta T . \tag{3-3}$$

Where $\langle k \rangle$ is the effective thermal conductivity of the insulation, b is the outer radius, and a is the inner radius of insulation.
A comparison of Eq. (3-3) with the conductive heat transfer equation, allows the definition of the effective cross-sectional area, A_{eff}, or radius, r_{eff}, as:

$$A_{eff} = 2\pi L\left(\frac{b-a}{\ell n \frac{b}{a}}\right) = 2\pi r_{eff} L \quad . \tag{3-4}$$

For inner and outer radii typically encountered with thermoelectric generators, the effective radius is very nearly $\frac{b+a}{2}$, i.e. the linear average of the inner and outer radii.

The conductive temperature drop between the radiator base and thermoelement cold junctions may be calculated by use of dimensions and properties of appropriate components and the total heat being transported. A reasonably good estimate of this temperature drop $\left(\Delta T_C\right)$ may usually be made. Temperature drops of the order of 20 to 40°C are typically calculated.

Not all of the heat rejected from a thermoelectric generator is transported by radiation and/or convection. Since the generator must be mechanically supported, a fraction, α, of the rejected heat is carried off by conduction through structural members. Usually this is only a small fraction of the total rejected heat, but for accuracy has to be taken into account. Similarly, for accuracy, it is also necessary to account for radiator emissivity, ϵ_r, and fin effectiveness, η_f, and the radiation view factor F.

The heat rejected by the radiator, Eq. (2-10), may be rewritten as

$$Q_{rej} = (1-\eta-\alpha)Q_{in} = A_R \sigma \epsilon_r \eta_f F\left(T_R^4 - T_{amb}^4\right) + KA_c\left(T_R - T_{amb}\right)^{\beta}, \tag{3-5}$$

Where all of the symbols have been previously defined.

The calculation of the effective convective and radiative areas of a thermoelectric generator, A_c and A_R respectively, is best illustrated by reference to Figure 2. The effective convective area, A_c, may in the first approximation be assumed to be given by the total external surface area of the generator. The effective radiative area, $A_R F$, may to the same approximation be assumed equivalent to the total equivalent area of the generator indicated by the dashed lines in Figure 2. This represents the minimum surface area required to enclose the RTG. The quantities α and η_f in Eq. (3-5) have also to be determined or approximated prior to the use of the equation to calculate the radiator base temperature T_R.

As already mentioned, Eq. (3-5) is solved by the Newton-Ralphson approximation.

Ignoring Thomson heat, the heat balance at the hot junctions of the thermoelements may be written as

$$Q_{radial} = \lambda Q_{in} = \left[\langle k_I \rangle A_e + N\langle k_n \rangle a_n + N\langle k_p \rangle a_p\right]\frac{\Delta T}{\ell} \qquad (3\text{-}6)$$

$$+ NI_S ST_H - 1/2NI_S^2 \delta \left(\frac{\langle \rho_n \rangle}{a_n} + \frac{\langle \rho_p \rangle}{a_p}\right)\ell ,$$

Where a_n and a_p are the cross-sectional areas of individual n- and p-type thermoelements, λ is fraction of total input heat that traverses the generator in the radial direction, δ accounts for extraneous circuit resistance and ρ_n and ρ_p are the electrical resistivities of the n-and p-type thermoelements. The definition of a total radial thermal conductivity, K_T, allows Eq. (3-6) to be rewritten as

$$\lambda Q_{in} = K_T \Delta T + \frac{\Gamma \Delta T}{(1+m)2}\left[T_H\ (1+2\,m) + T_C\right], \qquad (3\text{-}7)$$

where

$$K_T = \frac{N}{\ell}\left[\langle k_I \rangle \frac{A_e}{N} + \langle k_n \rangle a_n + \langle k_p \rangle a_p\right]$$

$$m = R_L / R_g$$

$$\Gamma = \frac{NS^2}{2\delta\left(\frac{\rho_n}{a_n} + \frac{\rho_p}{a_p}\right)\ell}$$

Note that R_L is the external load resistance and R_g is the internal generator resistance. Using the radiator temperature determined by Eq. (3-5) and recalling that

$$T_C = T_R + \Delta T_C \qquad (3\text{-}8)$$

allows solution of Eq. (3-7) for T_H.

Equations (3-5), (3-7), and (3-8) have been used to establish both the hot and cold junction temperatures. The non-integral power β and the efficiency term $(1-\eta)$ in Eq. (3-5) require two discrete iteration schemes in order to determine the temperatures of the generator. Because generator temperatures are not known a priori, it is necessary to start the calculational sequence by using arbitrary values of thermoelectric properties. As new temperatures are calculated in each iteration, an integration scheme is used to calculate average thermoelectric properties appropriate to these temperatures in each iteration.

PERFORMANCE CALCULATIONS

Once the thermoelement junction temperatures have been established, the performance of the generator is calculated in a straight-forward manner. The load voltage is given by:

$$V_L = \frac{m}{(1+m)} N_S S\Delta T \quad . \tag{3-9}$$

The power output may be written as:

$$P_{out} = \frac{m}{(1+m)2} \frac{NS^2\Delta T^2}{\delta R_i} \tag{3-10}$$

The load current is:

$$I_L = \frac{n}{(1+m)} \frac{S\Delta T}{\delta R_i} \tag{3-11}$$

Where m is the load ratio (R_L/R_g) and n is the number of parallel electrical branches in the generator. Generator conversion efficiency is given by:

$$\eta = P_{out}/Q_{in} \tag{3-12}$$

Because of the iterative nature of the calculational sequence outlined above, it is particularly convenient to effect the solution on a high speed computer. An example of the corresponding computer program, actually used to obtain the results discussed in Sections IV and V of this memorandum is reproduced in Appendix B.

IV. RCA MODULE EVALUATION

In order to test the validity of the mathematical model discussed in Sections II and III and, in some instances, to calculate thermal conductivities of selected thermal insulations, this section of the present memorandum deals with the calculation of the performance of RCA converters C-2, C-3 and C3Z, The calculated performance values are compared to the experimental data reported in References 6 and 7. The thermoelectric material used by all of these converters is a silicon-germanium alloy of composition 63 a/o Si - 37 a/o Ge in the conventional "Air-Vac" configuration with silicon-molybdenum alloy hot shoes. Both the n-and p-type thermoelements have a 0.0889 cm^2 cross-sectional area with an active length of 2.155 cm in all three converters. All converters employ eighteen thermocouples arranged electrically in series and have an hexagonal overall geometry. The thermal insulation in each converter has an effective area of 171 cm^2.

The temperature drop between the cold junction of the thermoelements and the radiator base is calculated to be approximately equal to 0.5 times the heat input. This figure is based upon approximate thermal resistances of the various components of the cold stack and the connection to the radiator surface. The primary difference between the three converters in question is the type of thermal insulation and the exact radiator configuration of each.

CONVERTER C-2

The C-2 converter employs multiple radiation/convection fins for waste heat rejection and uses Min-K 2020 thermal insulation. The radiation area of the radiator is calculated to be 817 cm^2, while the effective convective area is estimated to be about 1200 cm^2. The heat rejected from the radiator in vacuum is given by Eq. (3-5) with K set equal to zero. Using the RCA experimental data and the radiative area indicated above, Eq. (3-5) may be solved to give $\epsilon_r \eta_f F = 0.76$. This value may be expected to remain nearly the same for all the RCA generators considered in this report. Exact agreement in the cold side temperature (T_{COLD}), over the entire input power range, is noted in Fig. 3 for both vacuum and nitrogen environments. (Exact agreement is, of course, necessary at the P_{IN} =56 WATT vacuum point since the corresponding temperature was used to establish the value of $\epsilon_r \eta_f F = 0.76$.) In operation in an air

(nitrogen) environment, the convective heat flow is laminar and the gemetry dependent convective heat transfer coefficient, K, is calculated to be 2.38×10^{-4} watt/cm^2 - ^{o}K. The fraction, $1 - \lambda$, of heat lost from converter ends was assumed to be 0.05.

An effective value of thermal conductivity for the thermal insulation must be used in the calculation of thermoelement hot junction temperatures. The thermal conductivity of Min-K 2020 reported in Ref. 5 was used as a starting point. Inasmuch as the authors of the referenced report, express doubt about the validity of the reported values, these values of thermal conductivity were only used in the initial calculations and later adjusted to yield agreement between calculated and experimentally determined performance of the C-2 converter. As a result, the effective thermal conductivity of Min-K 2020 was found to be slightly greater in vacuum and slightly less in air than the values reported in Ref. 5. As seen in Fig. 3, exact agreement between the calculated and experimental hot junction temperatures was not achieved at the higher power input levels. Agreement between calculated and experimentally determined performance for the converter is however excellent (Fig. 4). This agreement is not surprising since it was the experimental power output of the converter that was used to back-calculate the values of effective thermal conductivity for Min-K 2020. Similar discrepancies in the thermoelement hot-junction temperatures were found to exist in the performances calculated for all of the RCA converters; this in spite of the fact that in some cases values of thermal conductivity back calculated by RCA were used. The small discrepancy between calculated and measured hot junction temperatures may possibly be partly attributed to the fact that the calculated temperatures refer to the actual hot-junctions whereas the measured temperatures most likely are dependent upon the location of the temperature sensors on the hot shoes. A small discrepancy in the thermophysical properties of the thermoelements may also result in some difference between calculated and experimental temperature values.

CONVERTER C-3

The C-3 converter employs six radiation fins for waste heat rejection and uses multi-foil thermal insulation. Effective areas of 719 cm^2 and 952 cm^2 were calculated respectively for the effective radiative and convective radiator areas. The product $\epsilon_r \eta_f F$ was again taken to be 0.76 and the convective heat transfer coefficient was again found to be 2.38×10^{-4} watt/cm^2 - ^oK. Converter C-3 is identical to C-2 except for the radiation/convection fins and the thermal insulation of the converter. The effective thermal conductivity of the multi-foil insulation in both nitrogen and vacuum was obtained from Ref. 6. Calculated thermoelement temperatures are shown in Fig. 5. Experimental data points measured at RCA are included for comparison. Other than the slight discrepancy in hot-junction temperatures which has already been mentioned, good agreement exist between calculated and measured data. Fig. 6 shows plots of converter power output and efficiency as functions of heat input. Good agreement between calculated and experimental data is again observed.

CONVERTER C-3Z

The C-3Z converter is identical to the C-3 except for the thermal insulation. Whereas converter C-3 employs multi-foil insulation, converter C-3Z uses Zircar (ZrO_2) instead. The absence of reported information on the effective thermal conductivity of Zircar in nitrogen necessitated a back-calculation from experimental performance data. Figs. 7 and 8 show plots of calculated thermoelement hot and cold junction temperatures and power output and efficiency for the C-3Z converter as functions of power input to the converter. As before, experimental data reported by RCA (Ref.7) are shown for comparison. The agreement between calculated and experimental data are once again on the whole quite good.

For convenience the back-calculated effective thermal conductivity values for the multi-foil, Zircar and Min-K 2020 thermal insulations in both nitrogen (air) and vacuum are plotted in Fig. 9. As already discussed, some of these back-calculated thermal conductivity data were obtained from RCA and some were an outcome of the present work.

V. MULTI-HUNDRED WATT GENERATOR EVALUATION

In evaluating the performance of the MHW-RTG, several distinct cases will be considered. Inasmuch as some question still exists on the type of thermal insulation to be used in the MHW generator, the present calculations have been performed for all three types of insulation considered in Section IV: the multi-foil, Zircar and Min-K 2020. The first case (Case I) is concerned with a generator geometry designed to optimize a RTG employing foil insulation which requires a thermoelement length of 0.8 inch. The generator is initially considered "open", thus, allowing direct exposure of the internal components when operated in air. In the second case (Case II), the generator has an approximate 18% increase in the thermoelement ℓ/A ratio to permit RTG performance optimization with fibrous insulation. Again the generator is initially considered "open". The generator configuration and dimensions used in the present analysis are those reported by GE at the MHW design review meeting, 10 December 1969, Washington D.C. The more important design parameters are tabulated for reference in Table 1.

By simply modifying the basic MHW design, it is possible to hermetically seal the RTG such that an inert gas may be contained within the generator during the air-operation phase. As will be seen, this eliminates many of the problems associated with generator operation in air. Although the generator exterior operates in air, the temperatures are low enough to avoid most problems associated with chemical reaction, etc. By selecting a low thermal conductivity gas, such as Xenon, the generator will deliver a significant amount of power in this "pre-launch" condition. After reaching the eventual vacuum environment of space, the generator could be vented to allow its performance level to be re-established at that corresponding to vacuum operation.

The use of inert gases in this application is presented by first considering the thermal conductivities of Argon, Helium, Krypton, and Xenon. The effect of these gases on the conductivity of insulation is then considered and finally the MHW-RTG performance is re-examined and a summary is provided (Tables II and III).

Case I Thermoelement Length = 0.8 inches

The generator is initially considered "open" and makes use of a silicon-germanium alloy with composition 80 a/o Si - 20 a/o Ge in the standard Air-Vac thermocouple configuration. The generator is a hexagon with conical end-caps. A schematic of the generator is shown in Fig. 10. The view factor, F, of the radiator has been assumed to be unity and the fin effectiveness has been set at 0.95 (Ref. 8) in the present analysis. It has been further assumed that 2.5 percent of the total heat input to the generator is lost through each end-cap; the remainder of the heat, less the power output, is rejected by radiation and/or convection. The radiator area, the same in this case for both radiative and convective heat transfer, includes the total lateral surface area of the generator and of one end-cap. The radiation area of the second end-cap has been discounted because in its intended application the generator will be mounted axially in tandem with another generator. A temperature differential of about 20°C has been calculated between thermoelement cold junctions and the radiator base by accounting for the thermal resistances of all cold stack members and the heat passed through each stack.

Using RCA supplied thermoelectric property data for the 80 a/o Si - 20 a/o Ge alloy, initial calculations of the foil insulated MHW generator performance in vacuum were conducted to test the applicability of the model. The results of this initial calculation are illustrated in Fig. 11. Calculated data reported by GE are shown as data points in the figure. Agreement between the performance calculated with the model described in this memo (using RCA property data) and the calculated performance values reported by GE is good. Although not shown in Fig. 11, similarly good agreement was obtained for the thermocouple cold junction temperatures. In view of certain questions regarding the thermoelectric property data reported by RCA for the 80 a/o Si - 20 Ge alloy, the calculation was repeated with the "1500 hour" property data of the alloy given in Memorandum #6 (Ref. 9). The results of that calculation are shown by the dashed curves in Fig. 11. It is noted that the agreement between GE data and the present data are no longer as good as before. The difference in the two sets of data is however, primarily due to the material properties and thus has little to do with the model being used. In fact,

the validity of the model has again been established by the close agreement of the GE data with those presently calculated when using identical thermoelectric properties. For purposes of consistency, however, all subsequent MHW generator performance calculations used the thermoelectric property data reported for the 80 a/o Si - 20 a/o Ge alloy in Ref. 9.

The hot and cold junction temperatures and performance of the multi-foil insulated MHW generator (thermoelement length = 0.8 inch) in air and vacuum operation are shown as functions of load current in Figs. 12 and 13. Generator performance in vacuum has assumed ambient heat sink temperatures of 0 and 311^{o}K. Only the latter heat sink temperature has been assumed for the air operation case. Although generator operating temperatures are dependent on the ambient heat sink temperature (see Fig. 12), the performance of the generator is practically independent of it. Thermoelectric properties and temperature differential across the thermoelements are minimally affected by small changes in generator radiator temperatures. The power output and load voltage as functions of load current (see Fig. 13) are the same for the 0 and 311^{o}K ambient heat sink temperatures. In addition to radiation, the air operation case has assumed heat rejection by natural convection; for the conditions of the MHW generator, the convective heat flow has been calculated to be laminar.

The hot and cold junction temperatures and performance of the Zircar-insulated MHW generator (thermoelement length = 0.8 inch) are shown as functions of load current in Figs. 14 and 15 for the same ambient heat sink conditions as assumed in connection with the foil-insulated generator. The corresponding data for the generator using Min-K 2020 thermal insulation are plotted in Figs. 16 and 17.

Case II Thermoelement Length = 1.2 inches

The results of the calculations performed with an increased thermoelement length of 1.2 inches (ℓ/A increased ~ 18%) are shown in Figs. 18 through 23 for the three different insulation materials. As indicated in Fig. 18, excessively high hot-junction

temperatures ($\sim 1200^{\circ}C$) result when the increased thermoelement length is used in conjunction with foil insulation. These high temperatures discount using foil insulation in this case.

On the other hand, the use of Zircar insulation with the increased length has resulted in performance (see Figs. 20 and 21) comparable to that calculated for foil-insulation with the smaller ℓ/A ratio. With the Zircar-insulation, maximum power is observed at a hot-junction temperature of $1125^{\circ}C$. In view of some recent experiments, this temperature is probably excessive for Zircar and some insulation decomposition into metallic components would result.

Figures 22 and 23 show the calculated performance of the increased thermoelement length generator using Min-K 2020 insulation. Improved performance is noted; but again, high temperature problems would most probably be encountered in vacuum operation because of excessive insulation temperatures.

The thermal conductivities of the insulations used in the calculation of the MHW performance are those plotted in Fig. 9. It should be noted that the air-operation calculations have thus made use of effective insulation thermal conductivity values in nitrogen. Although insulation thermal conductivity is probably slightly different in air than it is in nitrogen, the difference is not expected to be great. It should also be noted that the thermal conductivity of Min-K 2020 has to be extrapolated over a large temperature range (up to $1100^{\circ}C$) before it can be used in the vacuum calculations. This may introduce some error in the calculations if the conductivity deviates greatly from the projected behavior. The MHW generator operating temperatures and performances shown in Figs. 11 to 23 for air operation are however, believed to be reasonably accurate.

It should be noted that the performance of the "open" geometry MHW generator in going from vacuum to air operation is significantly reduced for all three thermal insulations considered. The biggest performance reduction occurs in the case of the multi-foil insulated generator, with the smallest reduction for the case of the generator that uses Min-K 2020 insulation. Vacuum performance, however, is greatest for the case of the multi-foil insulation and least for the Min-K 2020.

General Discussion of "Open" Generator Configuration

Of the two cases considered, the generator using the shorter thermoelement lengths (Case I) appears to give the most desirable overall performance. The high hot-junction temperatures encountered in Case II, would very likely cause insulation problems when the generator is operated in vacuum. Consequentially, the following discussion will be primarily directed towards the generator employing a thermoelement length of 0.8 inch. Whereas Figs. 12 to 17 show the relative temperatures and performances of the Case I MHW generator in air - and vacuum - operation for three different thermal insulations, the data in these Figures of course give no direct indication of potential problems that may arise as a result of the operating temperatures/environments in terms of damage to the generator. Considering first the case of the multi-foil insulated generator, it is noted that under open circuit operating conditions in vacuum the hot junction temperatures of the thermoelements approach the solidus temperature of the 80 a/o Si - 20 a/o Ge alloy (about 1300^{o}C). The fuel capsule temperature will in this case be of course correspondingly higher. It should be obvious that such a condition is undersirable from the standpoint of possible permanent damage due to a variety of effects associated with sublimation, chemical reactions, melting, sintering, etc. Every precaution should therefore be exercised to prevent the MHW generator from ever operating in an open circuit operating mode. In air operation the foil insulated MHW generator will exhibit thermoelement hot junction temperatures of the order of 800 to 900^{o}C. As regards silicon-germanium Air-Vac thermocouples, air operation at such temperatures is permissible without any deleterious effects. The cold side bonds to tungsten electrodes, as well as all other cold side components, should be able to withstand air operation for reasonable lengths of time at the indicated cold junction operating temperatures. Possible problems that may be encountered with the foil-insulated MHW generator are thus generally related to generator components other than those associated with the Air-Vac thermocouples. Probably the two main areas in which problems may occur are the multi-foil insulation itself and the graphite re-entry shell that encapsulates the fuel capsule in a RTG. At the indicated operating temperatures, refractory metals will severely oxidize in air and thus should not be

used in an unsealed MHW generator. Possible materials that may be used for the foil insulation if it is to operate in an air environment at elevated temperatures are nickel, platinum and various other nobel metals. Unfortunately, however, may of these metals are not compatible with silicon-germanium alloys at elevated temperatures because of relatively low temperature eutectic formations. Thus, for most non-refractory metal foil insulations to be used in silicon-germanium generators that operate at elevated temperatures, it is necessary to replace a portion of the inner foil insulation with fibrous-type insulations that are compatible with silicon-germanium alloys and that are designed for high temperature use. Although refractory metal foil insulations probably are compatible with silicon-germanium alloys at even the highest temperatures at which such alloys can be used, their sensitivity to oxidation precludes their use from unsealed silicon-germanium RTG's that will undergo air operation. In conclusion then, for refractory metal foil insulations to be used in high temperature silicon-germanium thermoelectric generators it is necessary that the inside of the system not be exposed to air during generator operation. If it is desired to operate an unsealed generator in air, it will be necessary to use non-refractory metal foil insulation or fibrous insulation. In the former case it will be necessary to use hybrid fibrous-foil insulation system to eliminate possible problems of interaction of the foil insulation with silicon-germanium alloys. As regards the use of a graphite re-entry shell to encapsulate the fuel capsule of a RTG, oxidation problems very definitely would occur at the indicated hot side operating temperatures if the system were to operate in air. The system would either have to be sealed or the graphite shell protected with an oxidation resistant coating in air operation.

As regards the fibrous insulations, Zicar (ZrO_2) and Min-K 2020 considered in the present analysis of MHW generator performance, it is noted that at the maximum power output operating point they both operate at temperatures compatible with their high temperature capabilities in both air and vacuum for the Case I thermoelement length of 0.8 inch. The case of the Min-K 2020 insulation in vacuum, however, is somewhat marginal in that its highest recommended

operating temperature is of the order of 1000°C. Under open circuit conditions with the MHW generator hot side vacuum operating temperatures in the 1100 to 1200°C range, it is believed that severe degradation problems will probably be encountered with both types of insulation. This condition will be even worse if the fibrous-insulated MHW generator is re-designed to operate at the maximum power point with a hot junction temperature of 1100°C (as in Case II). The points made in regards to possible oxidation problems of the graphite re-entry shell in air operation are also valid in the case of the fibrous insulated MHW generator. As before, no special problems are to be anticipated with the silicon-germanium Air-Vac thermocouples in either air or vacuum operation.

Enclosed Generator Employing Inert Gases

The introduction of a protective gas into the internal portion of the MHW generator reduces many of the forementioned problems associated with generator operation in an oxidizing environment. The analysis of this mode of operation follows that given in Ref. 10. The essential details of the analysis are discussed in the remainder of this section of the memorandum. To perform the analysis the thermal conductivity of Argon, Helium, Krypton and Xenon was determined, then the effect of the gas thermal conductivity upon the converter insulation was evaluated and finally the performance of the RTG was calculated.

Thermal Conductivity of Gases

The thermal conductivity of several gases of interest are shown in Fig.24. The solid lines represent experimental data for several of the gases. The dashed lines represent the calculated thermal conductivity using the technique given in Ref. 11. This technique used the Sutherland formula for computing the viscosity, μ, of a gas as:

$$\mu = \frac{5}{16\,\bar{\sigma}^2} \frac{(K\,MT)^{1/2}}{1 + \frac{S}{T}} \qquad (5\text{-}1)$$

Where $\bar{\sigma}$ is collision diameter of gas molecules, K is Boltzmann's constant, M is molecular mass, T is temperature, and S is the Sutherland's constant.

When the viscosity at one temperature, T_o, is known the Sutherland formula can be rewritten as

$$\mu = \mu_o \left(\frac{T}{T_o}\right)^{3/2} \left(\frac{T_o + S}{T + S}\right) \tag{5-2}$$

The product, $\frac{k}{\mu C}$, where k is the conductivity and C is the specific heat at constant volume, is practically independent of temperature. Thus for gases with a constant specific heat the conductivity varies as the viscosity. The difference between the calculated values and experimental values for air and nitrogen reflects the fact that the specific heat does vary somewhat with temperature, and that nitrogen is diatomic rather than monatomic, and in the case of air, it is a mixture rather than a pure gas. However, in the case of other gases good agreement between the calculated and experimental data is achieved (Ref. 12 and 13). All of the gas conductivity values are considered valid for pressures of about 0.1 to 2.0 atm.

Effect of Gas on Insulation Conductivity

As has been shown, the conductivity of various insulations of interest increase when used in a gas environment as opposed to a vacuum environment. The total conductivity of a material (insulator or otherwise) can be expressed as:

$$K = k_c + k_r + k_{con} \tag{5-3}$$

Where k_c is the contribution due to solid conduction, k_r is the contribution due to radiation, and k_{con} is the contribution due to convection. If the material is operated in a vacuum, then:

$$K = k_v = k_c + k_r \tag{5-4}$$

Where k_v is the effective conductivity in a vacuum. If a gas is then added, the conductivity becomes:

$$K = k_v + Ak_g \tag{5-5}$$

Where k_g = conductivity of the gas, and A = empirical constant. The value of the empirical constant A reflects the degree to which the conductivity of the gas is simple additive, i.e. superposition theory is valid, and the degree to which convective heat transfer may be occurring in the gas. Thus the value of A would depend upon the density of the insulation and the amount of open space within it. For example, in an insulation with a high pore volume, A would approach 1.0 if no convection is occurring. In a dense material with little or no pore volume, A would approach zero. In some cases where significant pore volume is present convection can be significant. In these cases the value of A could exceed 1.0.

Using Eq. (5-5) to evaluate A for various types of insulations based upon the curves shown in Fig. 9 and Ref. 14, it is found that for foil insulation, A varies from 1.0 to about 1.4. For Zircar, A varies from 0.7 to 1.0 and for Min-K, A varies from 0.4 to 0.75. Thus it appears that a significant amount of convection does occur in multifoil insulations whereas in the fibrous types the effect of convection is less severe. The high A value for foil insulation may also reflect some changes in the surface emissivity as the gas is absorbed (i.e.: $k_v \neq$ constant). This would be especially true in an oxidizing gas such as air. It should also be kept in mind that the use of Eq. (5-5) to evaluate the conductivity of insulations in gas requires the knowledge of the conductivity of the insulation in vacuum. As the conductivity of foil and fibrous type insulations are highly dependent upon edge effects in vacuum operation, these uncertainties will be reflected into the uncertainties of the conductivity when used in a gas.

Using average values for A, the effect of the gas conductivity upon the insulation conductivity has been plotted in Fig. 25. Notice that the effectiveness of the three insulations is reversed when operating them in air as opposed to vacuum. Operation in Krypton results in about the same conductivity for all three insulations. The points at which the conductivity of the gases are noted in Fig. 25 are based upon an average gas temperature typical of that encountered in the MHW generator employing thermoelement lengths of 0.8 inch (Case I). If the longer thermoelements were used (1.2 inch),

the average insulation temperatures would increase and as a result, the curves would be shifted upward by a significant amount. This would be particularly true in the case of Min-K, since the vacuum thermal conductivity is strongly temperature dependent. This increase in conductivity has been included in the performance calculations.

MHW Generator Performance Using Inert Gases

To obtain generality, the electrical performance of the MHW generator has been evaluated as a function of insulation thermal conductivity. For the two generators considered, Case I - thermoelement length = 0.8 inch and Case II - thermoelement length = 1.2 inch, the performance is shown in Fig. 26. The sink temperature was held at 311^{o}K for all cases investigated. However, as has been shown, the power output does not significantly depend upon the sink temperature and therefore the output power can be shown as a function of insulation conductivity alone. The behavior is illustrated in the figure. Shown are the peak power and the power at a load voltage of 30 volts. Note that the power at 30 volts coincides with the peak power for the 0.8 inch element lengths (Case I) at insulation conductivities corresponding generally to operation in vacuum; whereas, the 30 volt power coincides with peak power for element lengths of 1.2 inch at conductivity values corresponding to operation in air.

Just as the power output is independent of sink temperature it is also independent of RTG external environment, This is not true for the RTG temperatures. The temperatures depend both upon the sink temperature and the presence or absence of gases external to the RTG. For all cases evaluated using an internal vacuum environment, the external environment was also considered to be a vacuum. For all cases using a gaseous internal environment, air was assumed to be the external environment. The gas pressures were assumed to be about 1 atm.

Fig. 27 shows the hot and cold junction RTG temperatures as a function of insulation conductivity. The temperatures at open circuit, peak power, and short circuit are identified. The data shown in Fig. 27 are for a thermoelement length of 0.8 inch (Case I). Fig. 28 shows the temperatures for the case of a thermoelement

length of 1.2 inch (Case II). As would be expected the hot junction temperatures for the longer element length are significantly higher as the length to area ratio is about 18% higher for that case. The cold junction temperatures are essentially the same for both element geometries.

The hot junction temperature at a load voltage of 30 volts may be either higher or lower than the temperature at peak power depending upon the particular insulation conductivity and element geometry. As shown in Figs. 29 and 30 the 30 volt power may lie either to the short circuit or open circuit side of the peak power current. In general, for the 0.8 inch element length, the 30 volt power lies to the open circuit side of peak power for the high conductivity insulation; for the 1.2 inch element length, the 30 volt power points lie to the short circuit side of peak power. Thus for the 0.8 inch element length, the 30 volt hot junction temperatures may be somewhat greater than the peak power temperatures and for 1.2 inch element length the 30 volt hot junction temperatures will probably be less than the peak power temperatures.

A summary of the peak power output, 30 volt power output, hot and cold junction temperatures at peak power is given in Tables II and III for the various insulations and gases that were considered in this study. In vacuum and low conductivity gases, foil gives the best performance and Min-K the poorest. For air and other gases of comparable conductivity Min-K gives the best performance while the foil gives the poorest. For all cases Zircar gives performance in between foil and Min-K. See pp. 19 and 20 for comments regarding RTG operating temperatures.

Two points worthy of further consideration should be mentioned. First, as was pointed out, the vacuum performance of foil and fibrous insulations is highly dependent upon end losses and thus the geometry of the converter. Consequently, a detailed analysis of the MHW-RTG geometry with respect to this problem needs to be carried out to ascertain the validity of the vacuum values of conductivity used in this study. Secondly, the computer program used in this study considered the RTG end losses to be fixed. In general, if the RTG is operated in a gas the end losses will increase by an amount dependent upon the conductivity of the gas. Thus the power output and the hot junction temperatures will be somewhat lower than shown here. The magnitude of this difference needs to be examined.

SUMMARY

The present study has been concerned with air/inert gas operation of thermoelectric generators designed for vacuum operation. The object of the study has been the development of a model to determine gas and vacuum performance of such generators. The validity of the model has been verified by its applications to several existing generators which have been tested in both vacuum and air (actually nitrogen) environments. The model has also been used to back-calculate the thermal conductivities of selected thermal insulations that presently are considered for use in high temperature silicon-germanium RTG's. Finally the model has been applied to the MHW generator, with two different thermoelement lengths, to determine its' performance under various environmental conditions. The initial characterization was performed in vacuum and then the effects of various inert gases upon the insulation conductivity were included. The calculations were performed with three different thermal insulations: multifoil, Zircar and Min-K 2020. Conclusions drawn from the latter evaluation may be summarized as follows:

1. The foil insulated MHW generator employing 0.8 inch thermoelements exhibits some 54 percent of its peak-power vacuum performance in air operation. Use of 1.2 inch thermoelements in foil-insulated generator results in excessive temperatures. The MHW generator insulated with Zircar exhibits some 59 percent for Case I and 75 percent for Case II of its peak-power vacuum performance in air operation; while, the corresponding percentages, for the Min-K 2020 insulated generator are 73 percent and 89 percent for the Case I and Case II respectively.

2. For fixed generator design, foil insulation yields the best peak-power vacuum performance for the MHW generator. Zircar insulation gives an intermediate performance level; while, Min-K insulation gives the lowest performance.

3. No permanent damage to the Air-Vac thermocouples used in the MHW generator is anticipated as a result of air operation with any of the internal gases considered.

4. If the MHW generator is permitted to operate in an open-circuit operating mode in vacuum, excessive hot side operating temperatures will probably cause permanent damage to the Air-Vac thermocouples and also the thermal insulation and possibly to the fuel capsule.

5. The use of foil insulations in the MHW generator requires special consideration when planning to have an "open" generator operate both in air and vacuum. Refractory metal foils are suitable for vacuum operation but cannot be used in an unsealed generator that also operates in air. Nickel, platinum and other noble metal foils can operate in both air and vacuum but at elevated temperatures are incompatible with silicon-germanium alloys because of relatively low temperature eutectic formations.

6. No incompatibility problems exist with the fibrous insulations (Zircar and Min-K 2020) up to hot side operating temperatures of the order of 1000^{o}C in both air and vacuum. At the higher temperatures encountered in Case II, however, these insulations may experience shrinkage, decomposition and/or interaction with silicon-germanium alloys.

7. If a protective gas is used inside the generator, the refractory foil offers the most advantageous insulation system.

8. The graphite re-entry shell of the radioisotope fuel capsule in the MHW generator will operate at elevated temperatures. If the capsule is to operate in air it will be necessary to keep the shell from being oxidized.

In conclusion it may be stated that probable problem areas in the unsealed air operation of the MHW generator relate to the graphite re-entry shell of the fuel capsule and the foil insulation, if foil insulation that employs refractory metals is used in the generator. Both problem areas may be conveniently eliminated by sealing the generator and employing inert gases during air operation. If forced convection is used instead of the natural convection assumed in the present investigation, it may be possible to significantly decrease all generator operating temperatures. Although this procedure would somewhat alleviate some potential problem areas associated with the air operation of the "open" MHW generator, it would be by no means eliminate them.

TABLE I

Characteristics of MHW-RTG Preliminary Reference Design

As Described by General Electric

RTG	
PERFORMANCE	
POWER	148 WATTS BOM 114 WATTS EOM (12 YR)
VOLTAGE	30 VOLTS DC
FUEL LOADING *	2000 WATTS (2-1000 WATT HEAT SOURCES)
$T_{HOT\ JUNCTION}$	$1100^{\circ}C$ ($2012^{\circ}F$) BOM
$T_{COLD\ JUNCTION}$	$335^{\circ}C$ BOM ($635^{\circ}F$)
CONVERSION EFFICIENCY	7.4 % BOM
GEOMETRY	
DIAMETER *	11.85" ACROSS DIAGONALS (HEX)
LENGTH *	20.0"
CONFIGURATION *	6 SIDE STRUCTURE - NO FINS
CONVERTER	
END CLOSURES	SPOKED TITANIUM
LOAD STRUCTURES	6 TITANIUM LONGERONS
RADIATORS	BERYLLIUM-IRON TITAN. COATING $\epsilon \approx 0.85$
THERMOELECTRIC COUPLES	
NUMBER *	288 (SERIES PARALLEL)
MATERIAL *	SiGe (80% SILICON)
LEG DIMENSIONS * (Case I)	N-LEG 0.8" LONG x .0188 IN^2 P-LEG 0.8" LONG x .0208 IN^2
LEG DIMENSIONS * (Case II)	N-LEG 1.2" LONG x .0238 IN^2 P-LEG 1.2" LONG x .0262 IN^2
HOT SHOES	SiMo
INSULATION *	LINDE-TYPE FOIL, ZIRCAR, MIN-K 2020

* Input data for performance calculations

TABLE 2 MHW-RTG Performance in Vacuum and Gas Environments for Thermoelement Length of 0.8 in.

FOIL INSULATION						
GAS	VAC	HELIUM	AIR	ARGON	KRYPTON	XENON
$P_{Max,}$ Watt	138	17	69	84	106	118
$P_{30V,}$ Watt	137	-	56	80	105	117
$T_{H,}$ °C *	1065	543	810	872	939	972
$T_{C,}$ °C *	321	282	279	278	276	275
ZIRCAR INSULATION						
$P_{Max,}$ Watt	124	24	73	88	103	111
$P_{30V,}$ Watt	123	-	61	85	101	109
$T_{H,}$ °C *	1012	591	844	885	929	950
$T_{C,}$ °C *	323	282	279	278	277	276
MIN-K 2020 INSULATION						
$P_{Max,}$ Watt	116	35	84	94	103	108
$P_{30V,}$ Watt	115	-	77	91	101	106
$T_{H,}$ °C *	986	652	860	903	929	941
$T_{C,}$ °C *	323	281	279	278	277	277

* Temperatures are for maximum power points

TABLE 3 MHW-RTG Performance in Vacuum and Gas Environments for Thermoelement Length of 1.2 in.

FOIL INSULATION						
GAS	VAC	HELIUM	AIR	ARGON	KRYPTON	XENON
$P_{Max,}$ Watt	161	28	92	114	135	145
$P_{30V,}$ Watt	155	-	91	114	132	140
$T_{H,}$ °C *	1195	641	934	1016	1070	1100
$T_{C,}$ °C *	320	282	277	276	274	273
ZIRCAR INSULATION						
$P_{Max,}$ Watt	135	37	101	110	123	130
$P_{30V,}$ Watt	134	8	101	110	122	128
$T_{H,}$ °C *	1125	700	970	1002	1039	1057
$T_{C,}$ °C *	321	281	277	276	275	275
MIN-K 2020 INSULATION						
$P_{Max,}$ Watt	123	51	110	105	112	115
$P_{30V,}$ Watt	122	32	110	105	112	114
$T_{H,}$ °C *	1102	774	1004	987	1006	1015
$T_{C,}$ °C *	322	280	276	276	276	276

* Temperatures are for maximum power points.

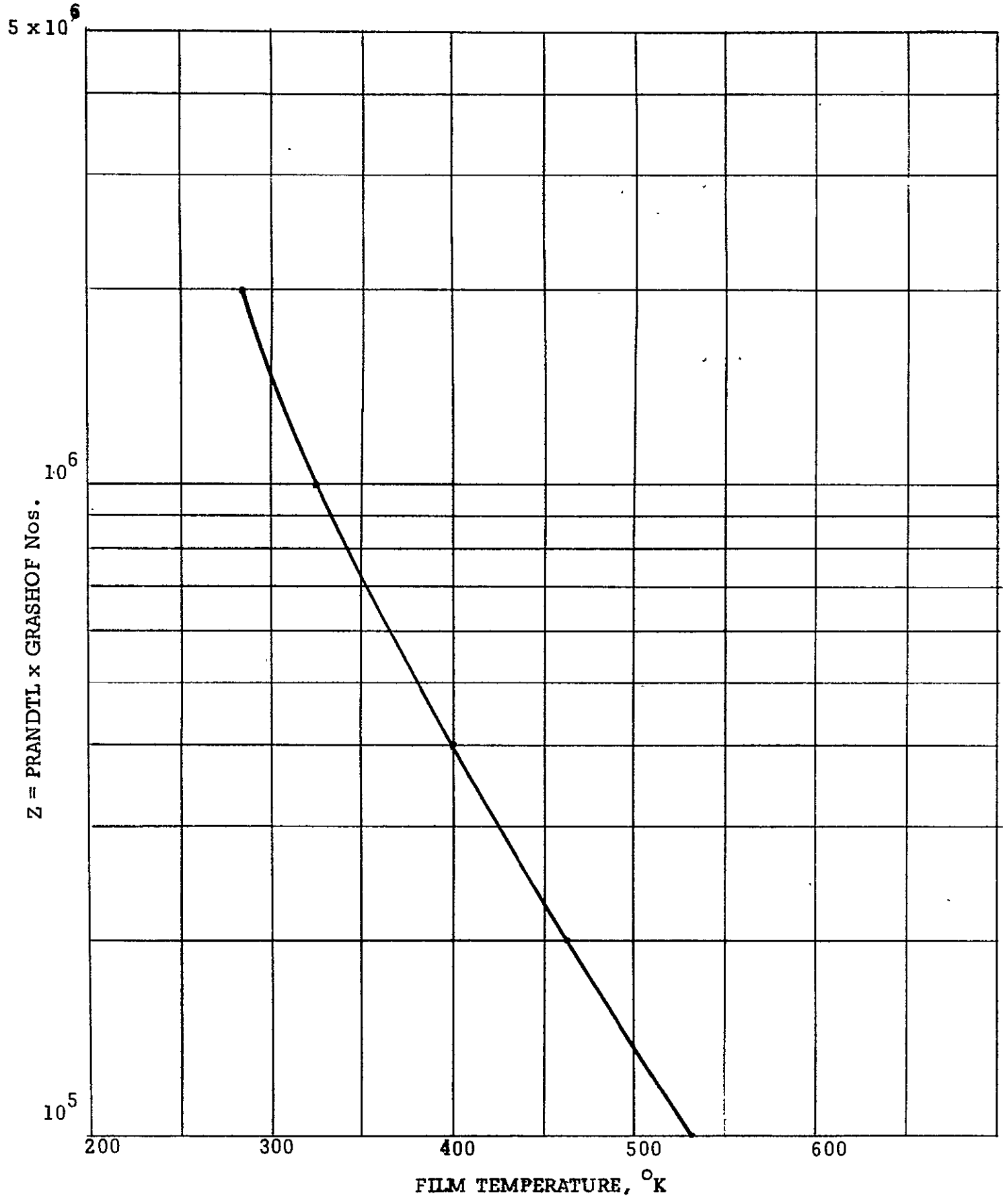

Fig. 1 Chart for Determining the Value of Z

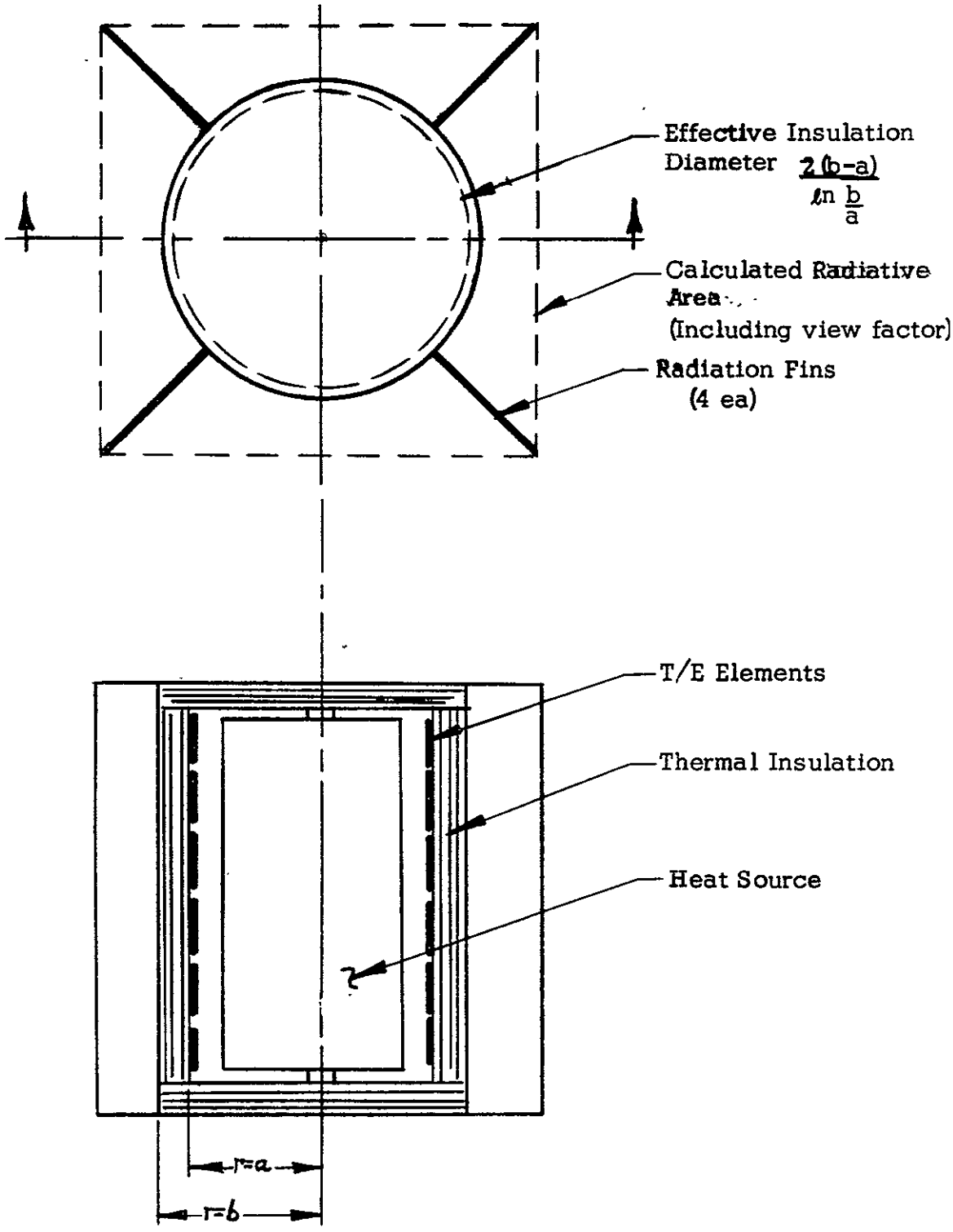

Fig. 2 Typical Generator Configuration

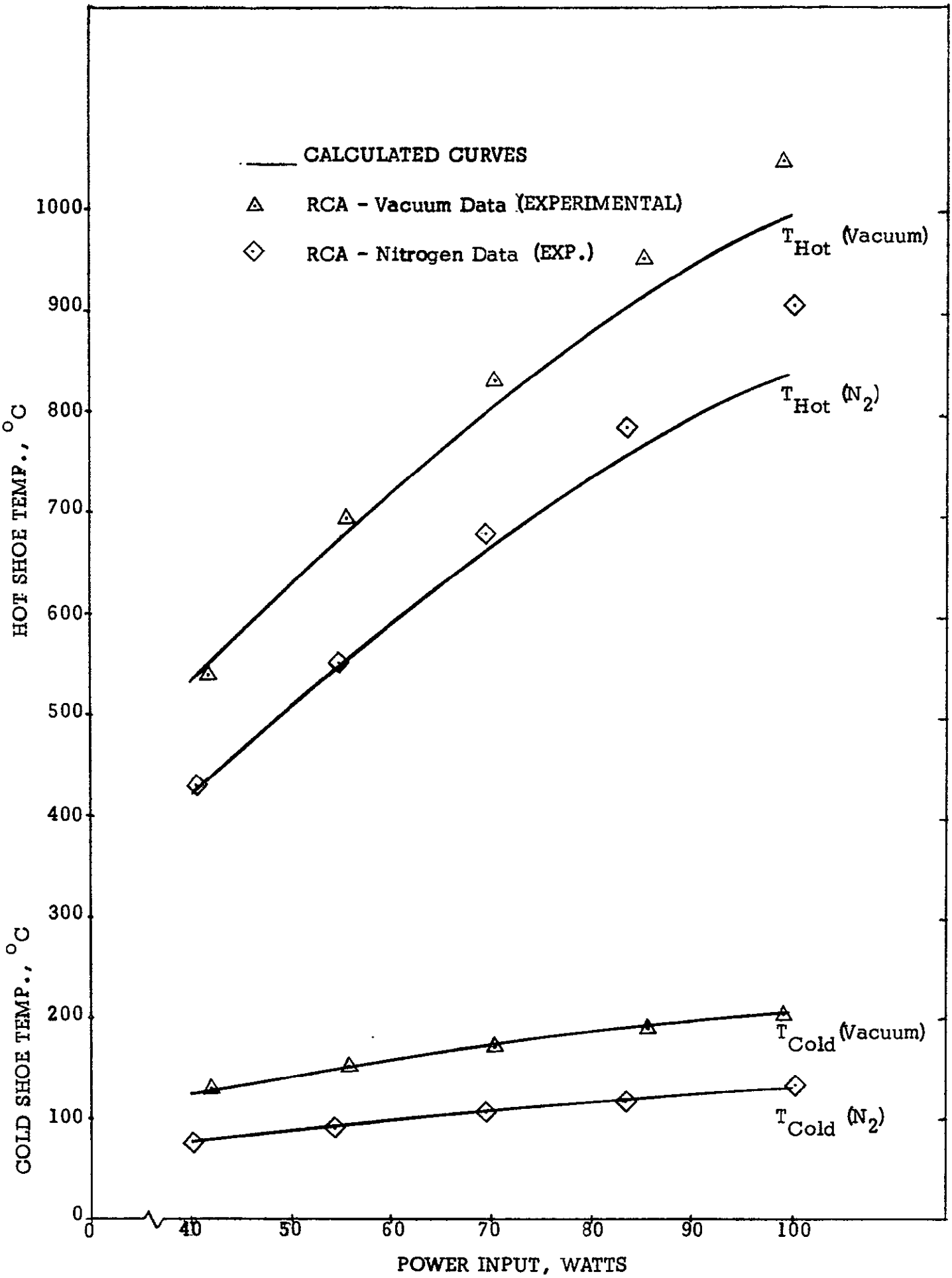

Fig. 3. C-2 Min-K 2020 Insulated Converter Vacuum/Nitrogen Performance

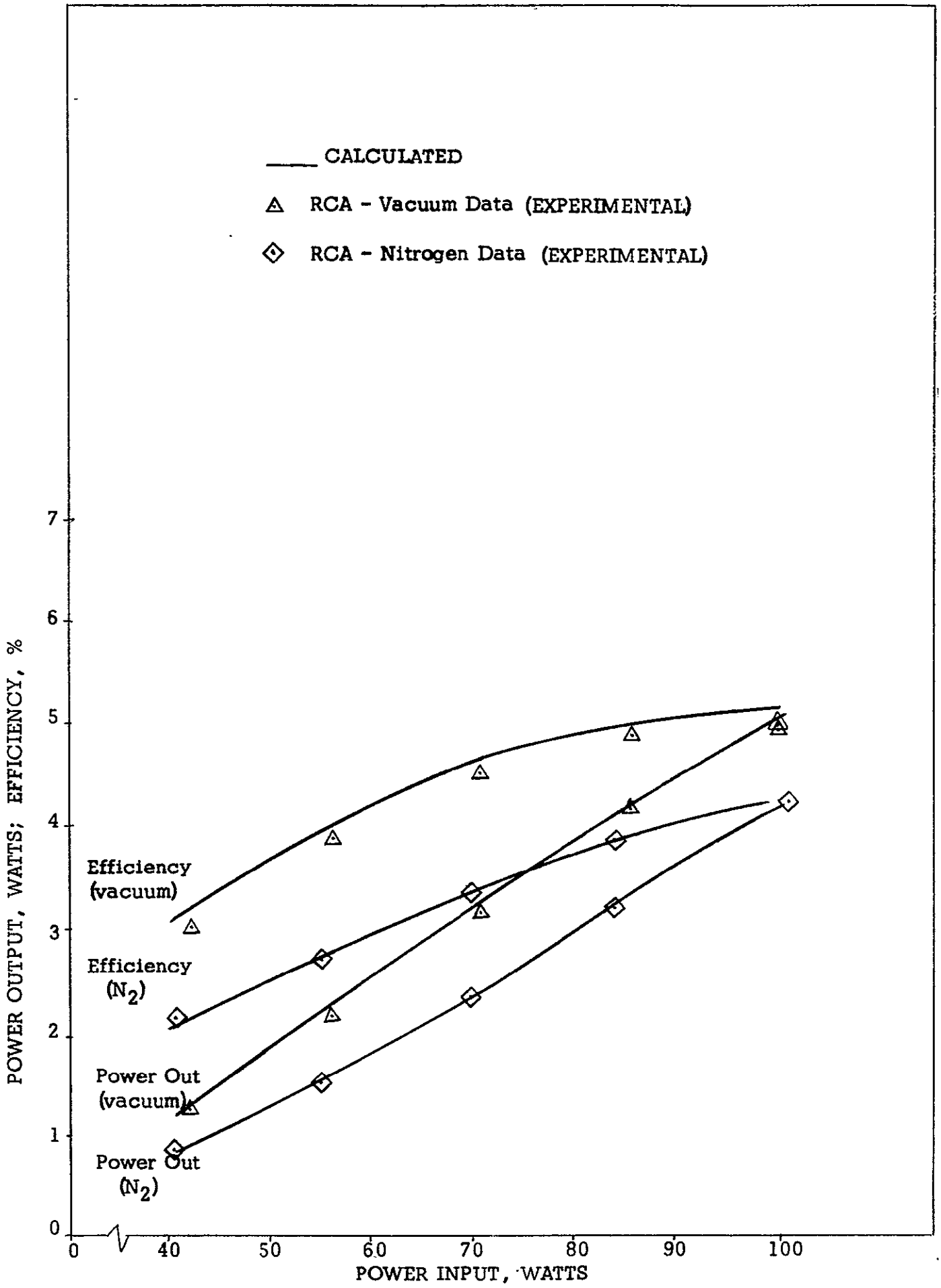

Fig. 4 C-2 Min-K2020 Insulated Converter Vacuum/Nitrogen Performance

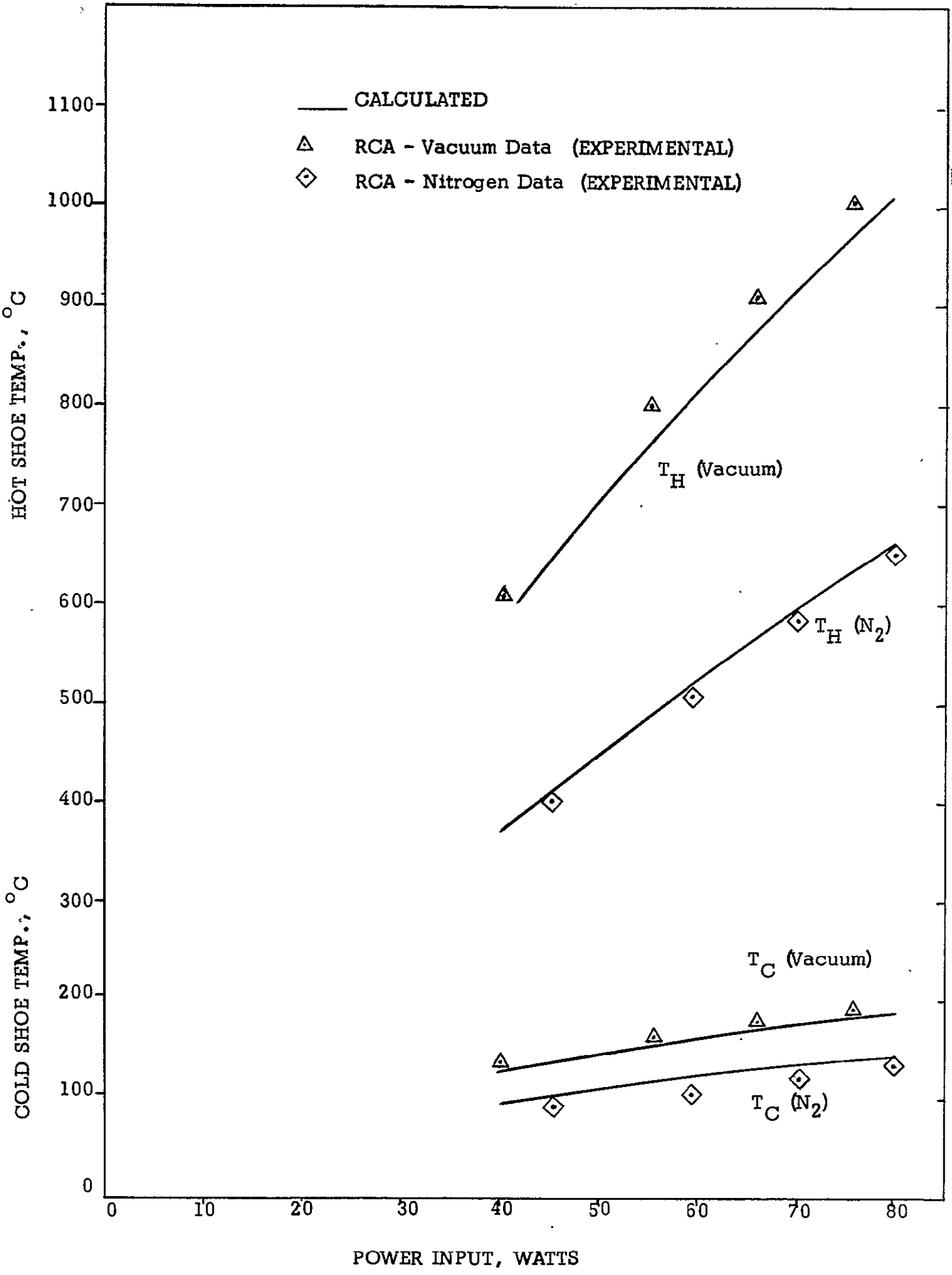

Fig. 5 C-3 Foil Insulated Converter Vacuum/Nitrogen Performance

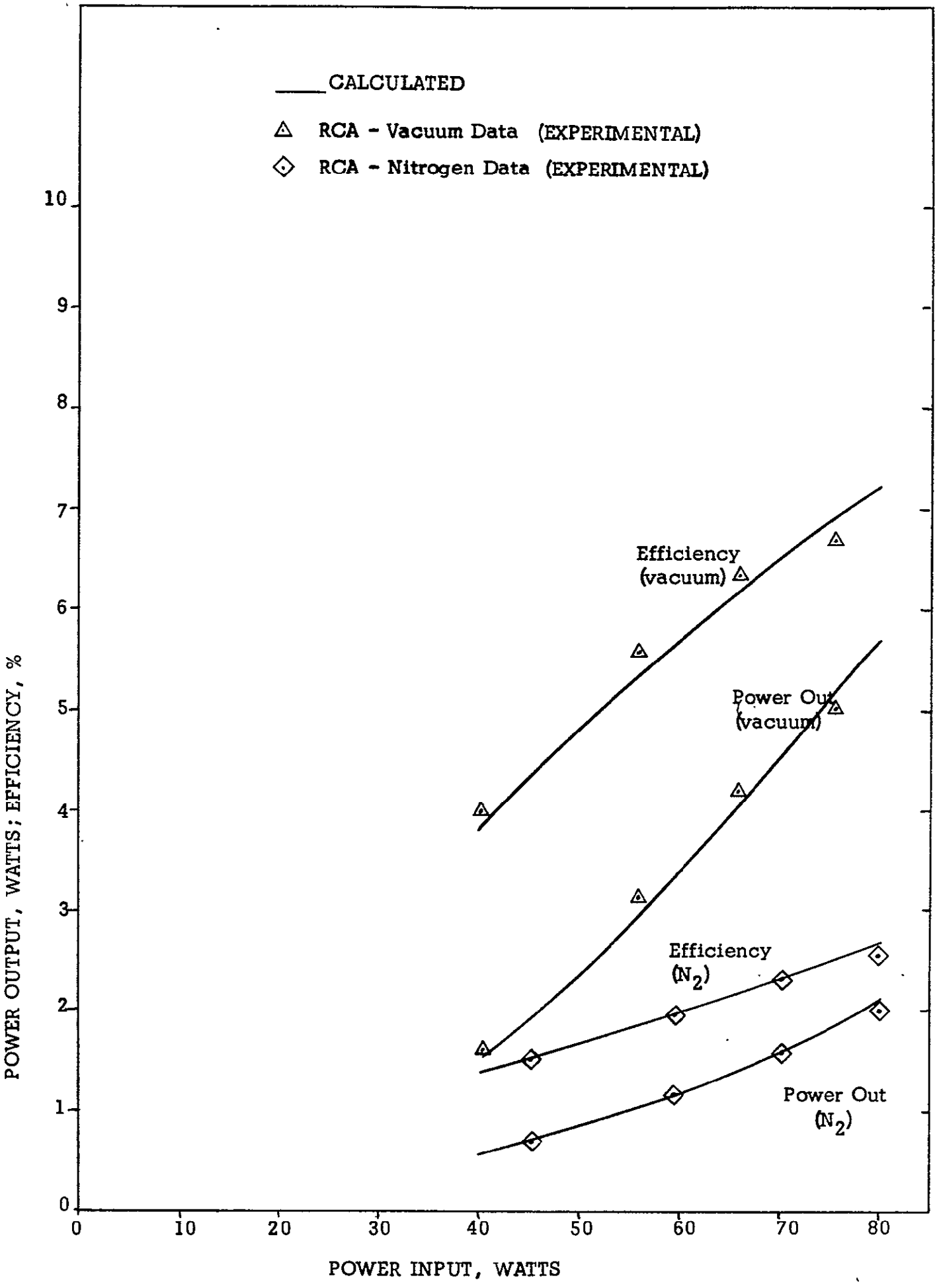

Fig. 6 C-3 Foil Insulated Converter Vacuum/Nitrogen Performance

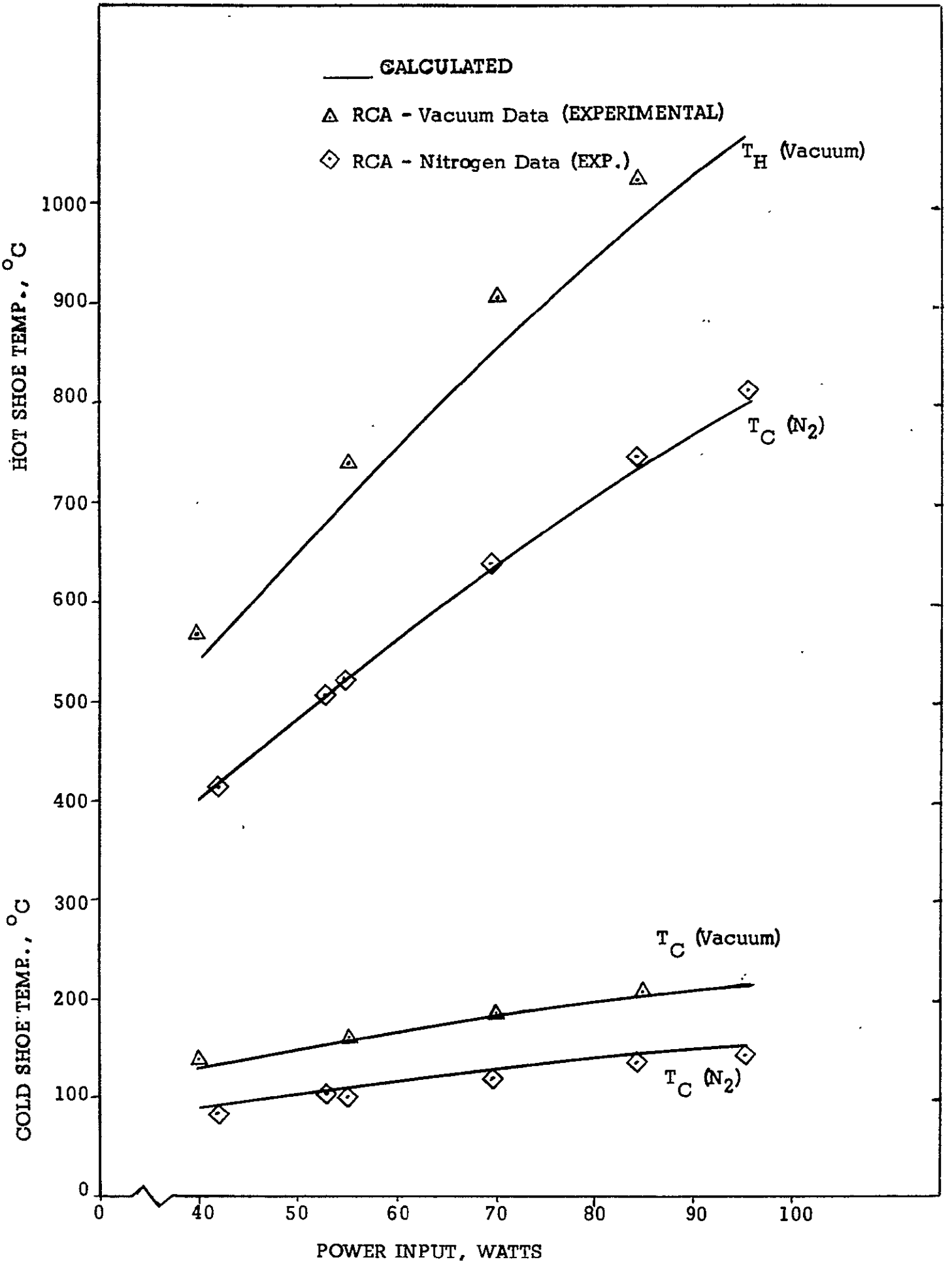

Fig. 7 C-3Z ZrO_2 Insulation Converter Vacuum/Nitrogen Performance

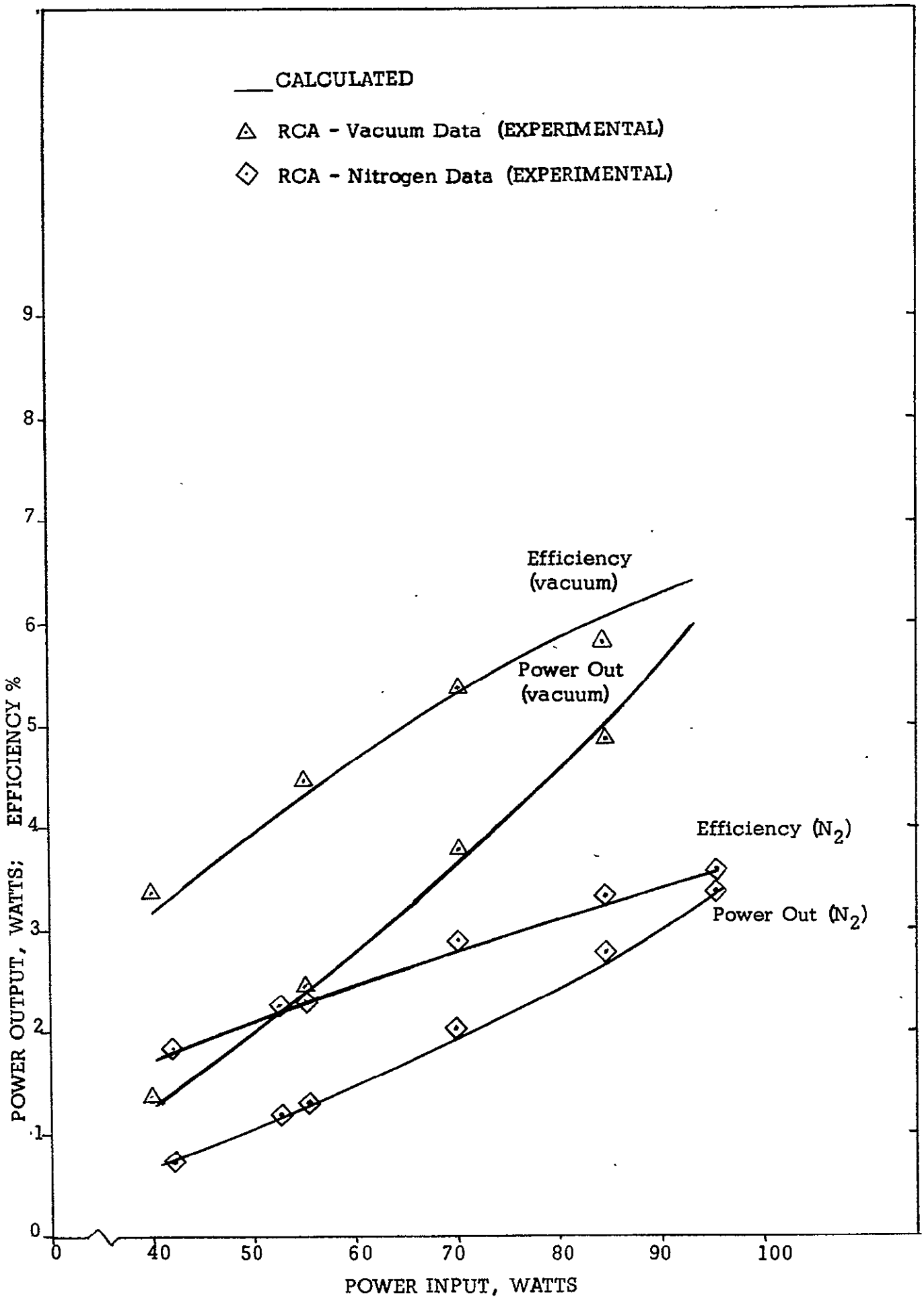

Fig. 8 C-3Z ZrO_2 Insulation Converter Vacuum/Nitrogen Performance

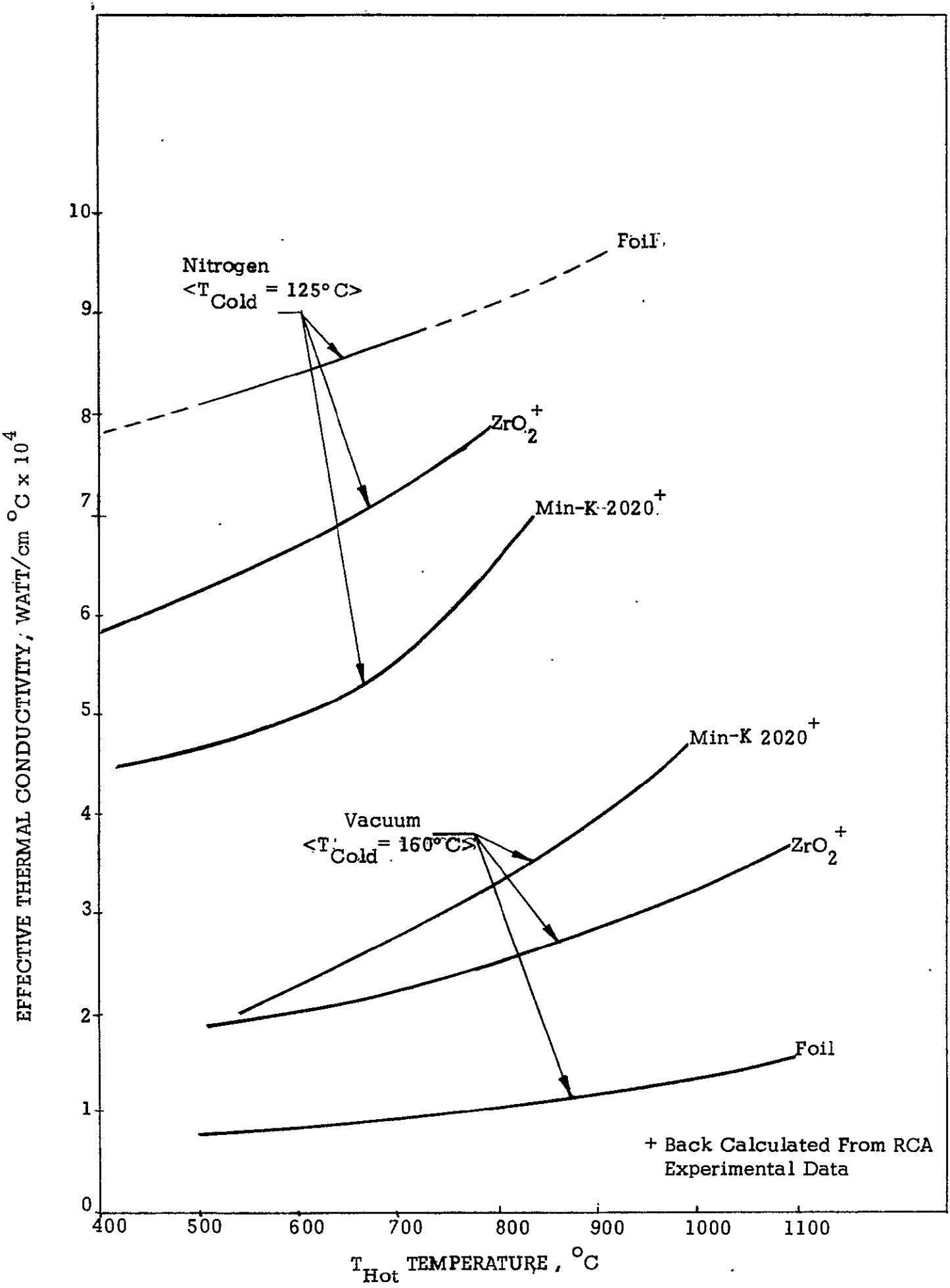

Fig. 9 Effective Thermal Conductivity in Vacuum and Nitrogen

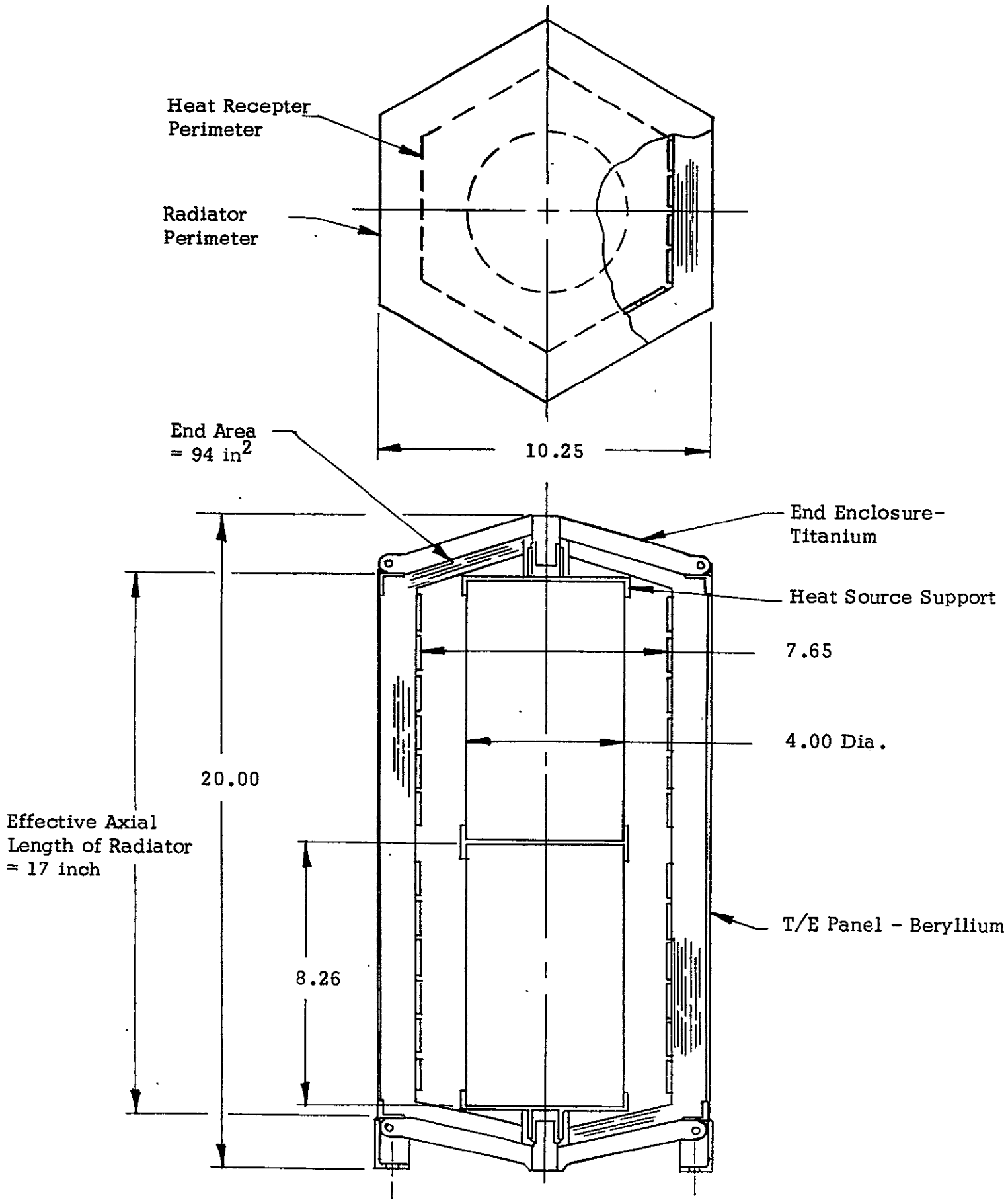

Fig. 10 MHW RTG Preliminary Design

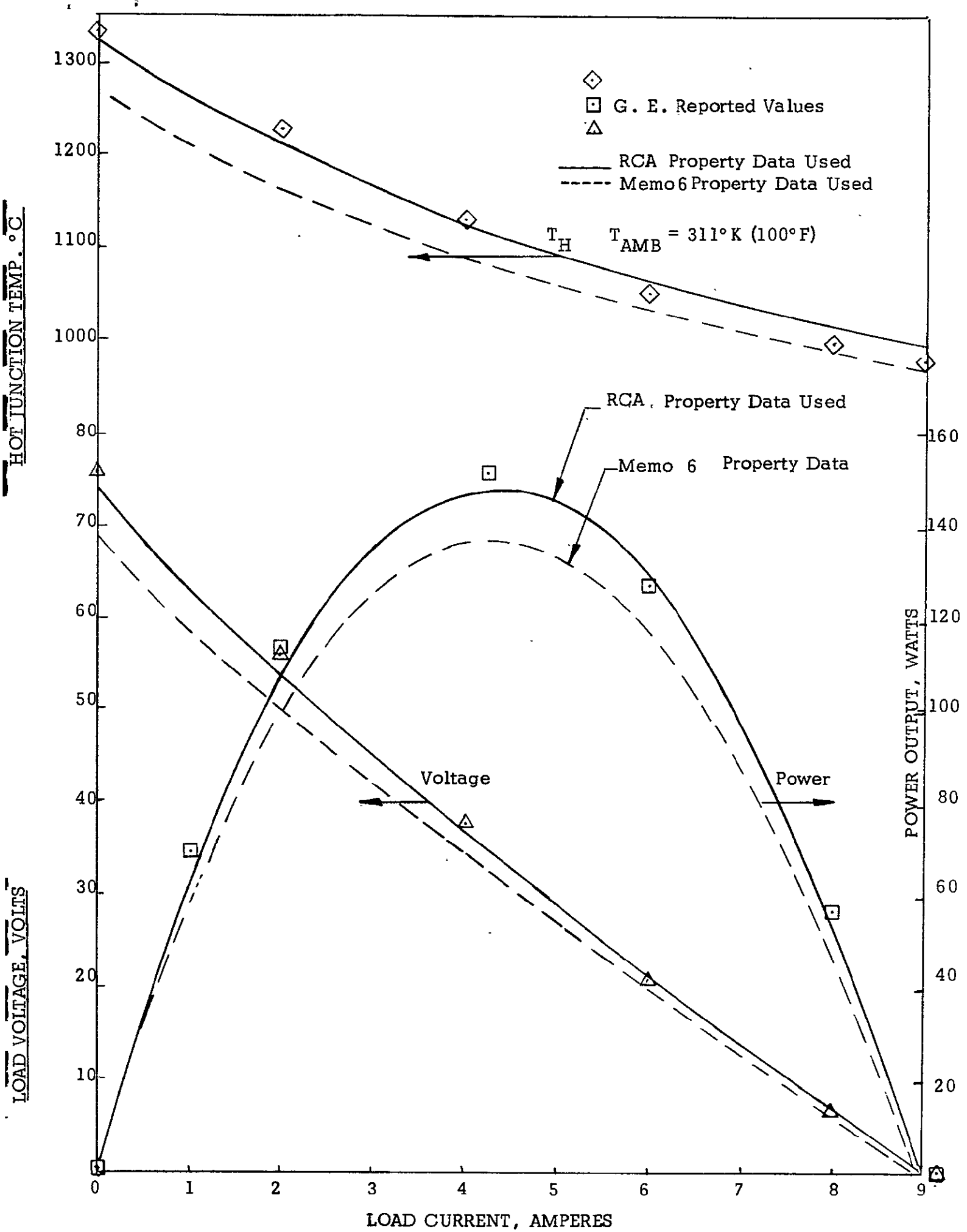

Fig. 11 MHW Comparative Performance

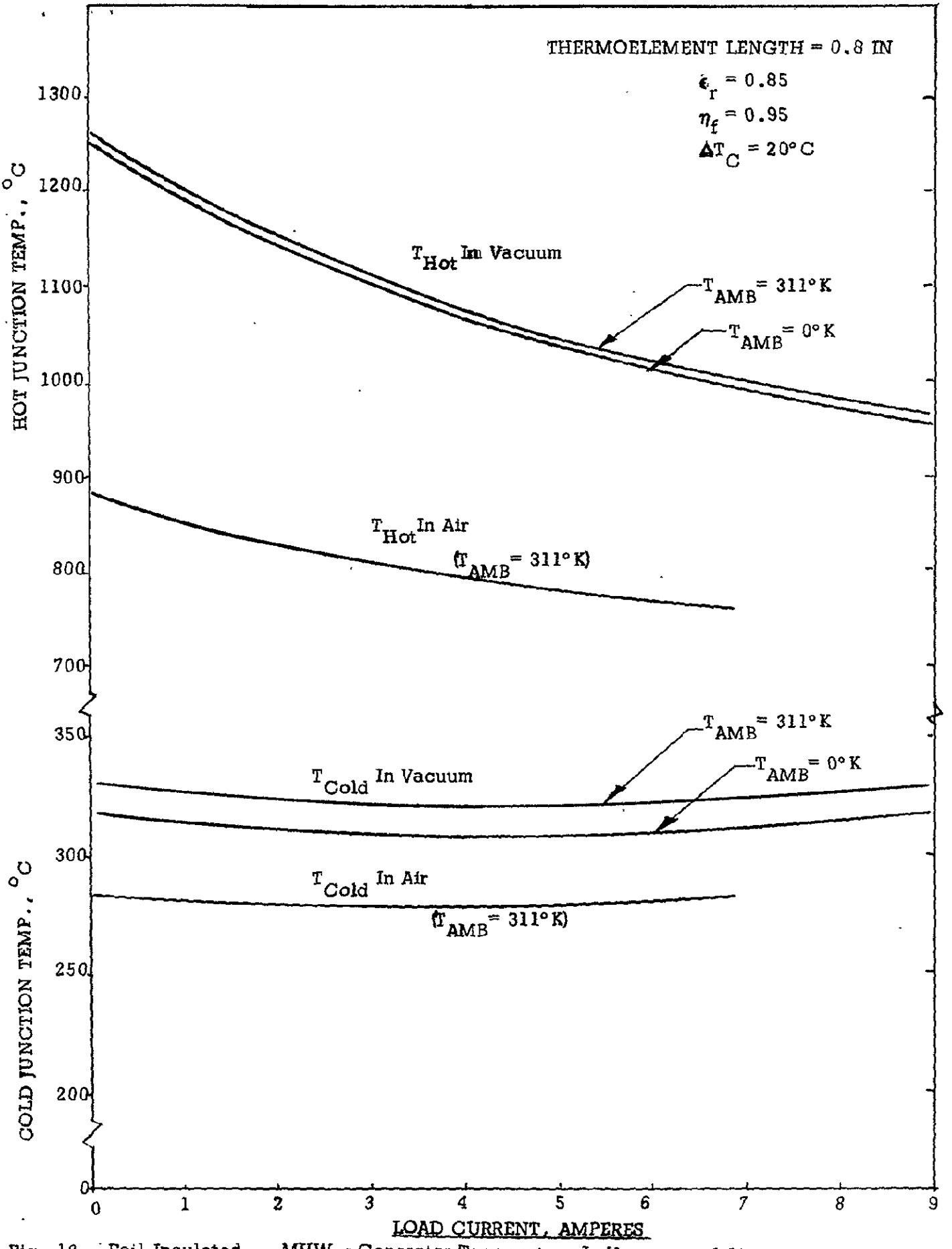

Fig. 12 Foil Insulated MHW - Generator Temperature In Vacuum and Air

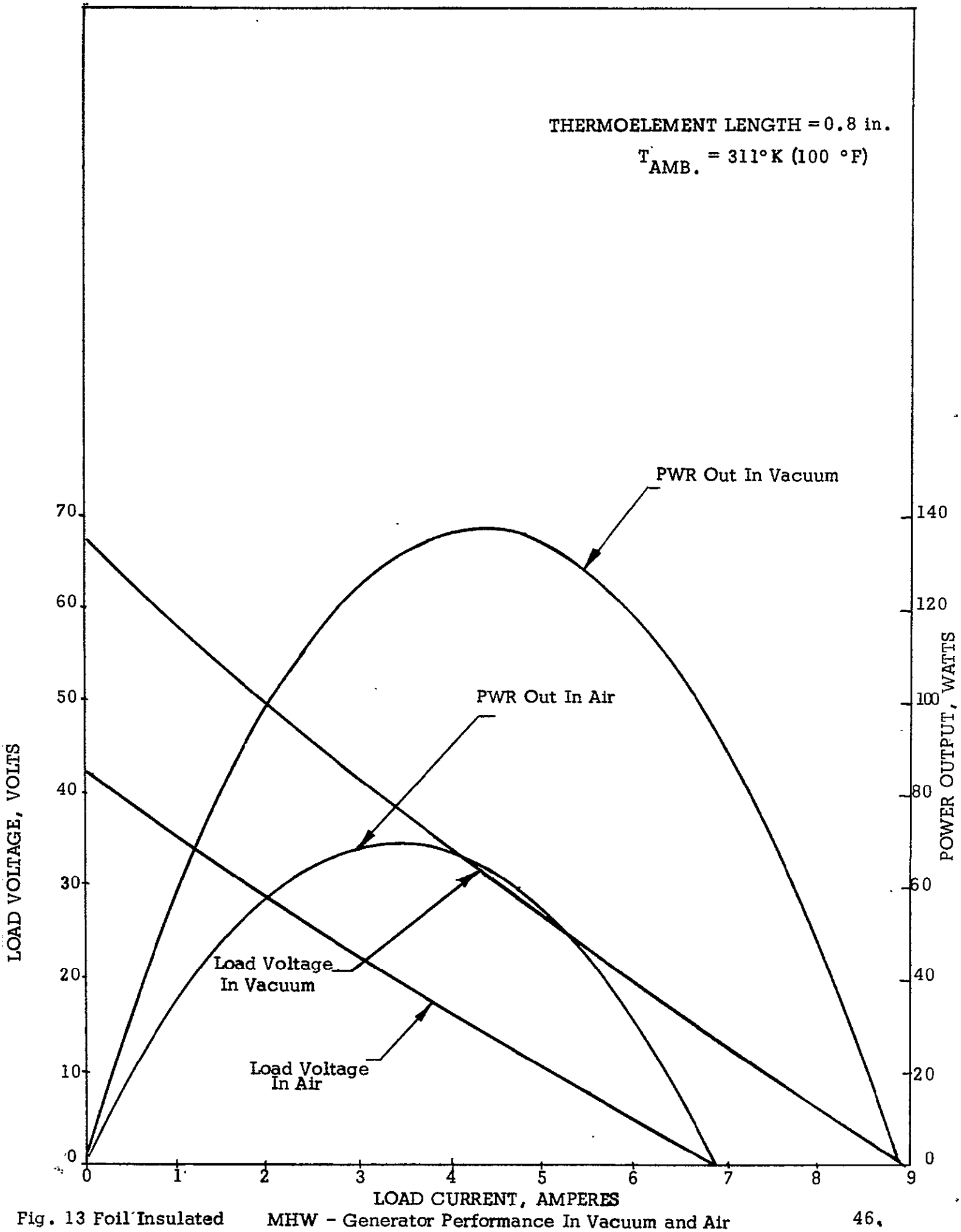

Fig. 13 Foil Insulated MHW - Generator Performance In Vacuum and Air

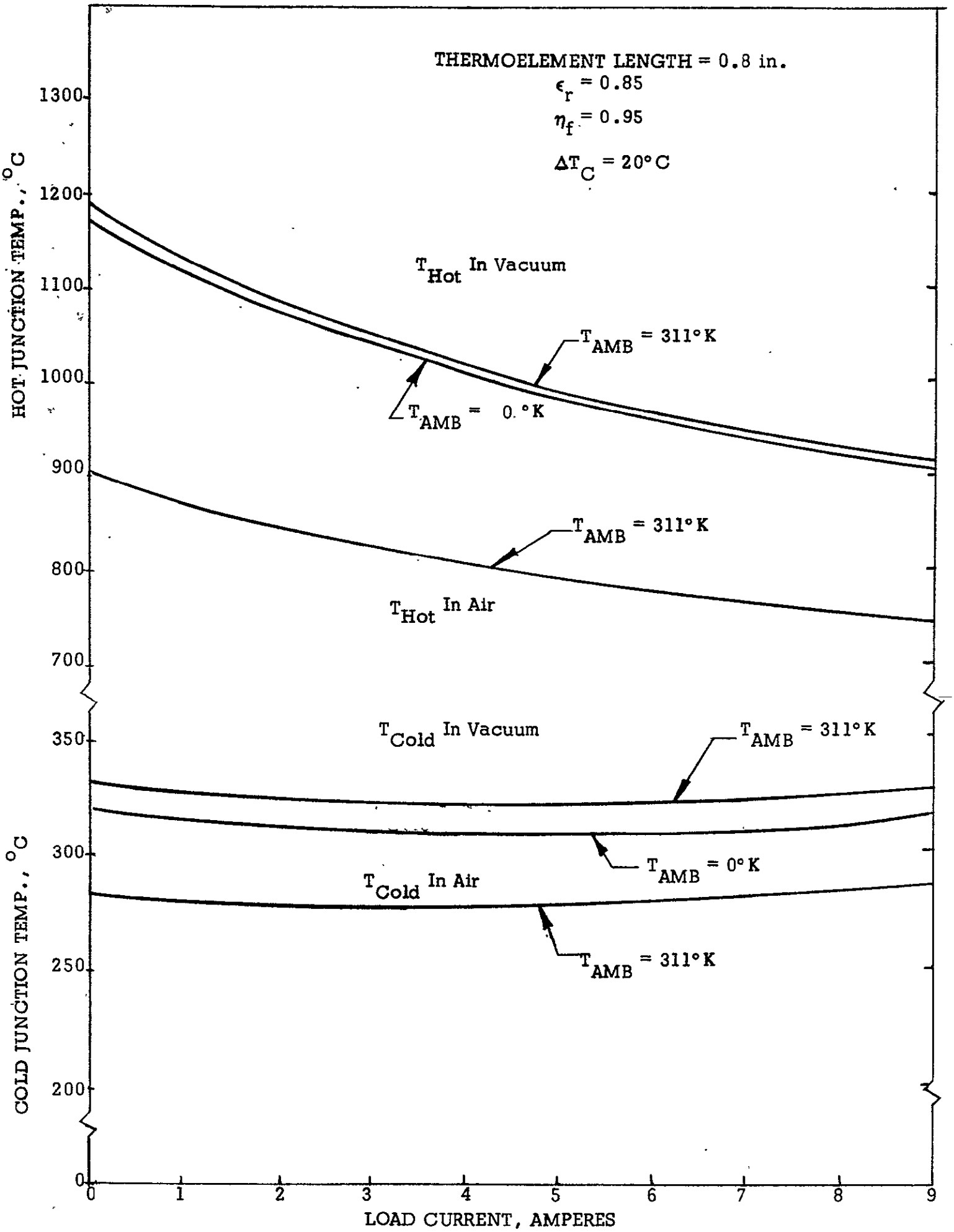

Fig. 14 ZrO_2 Insulated MHW - Generator Temperature In Vacuum and Air

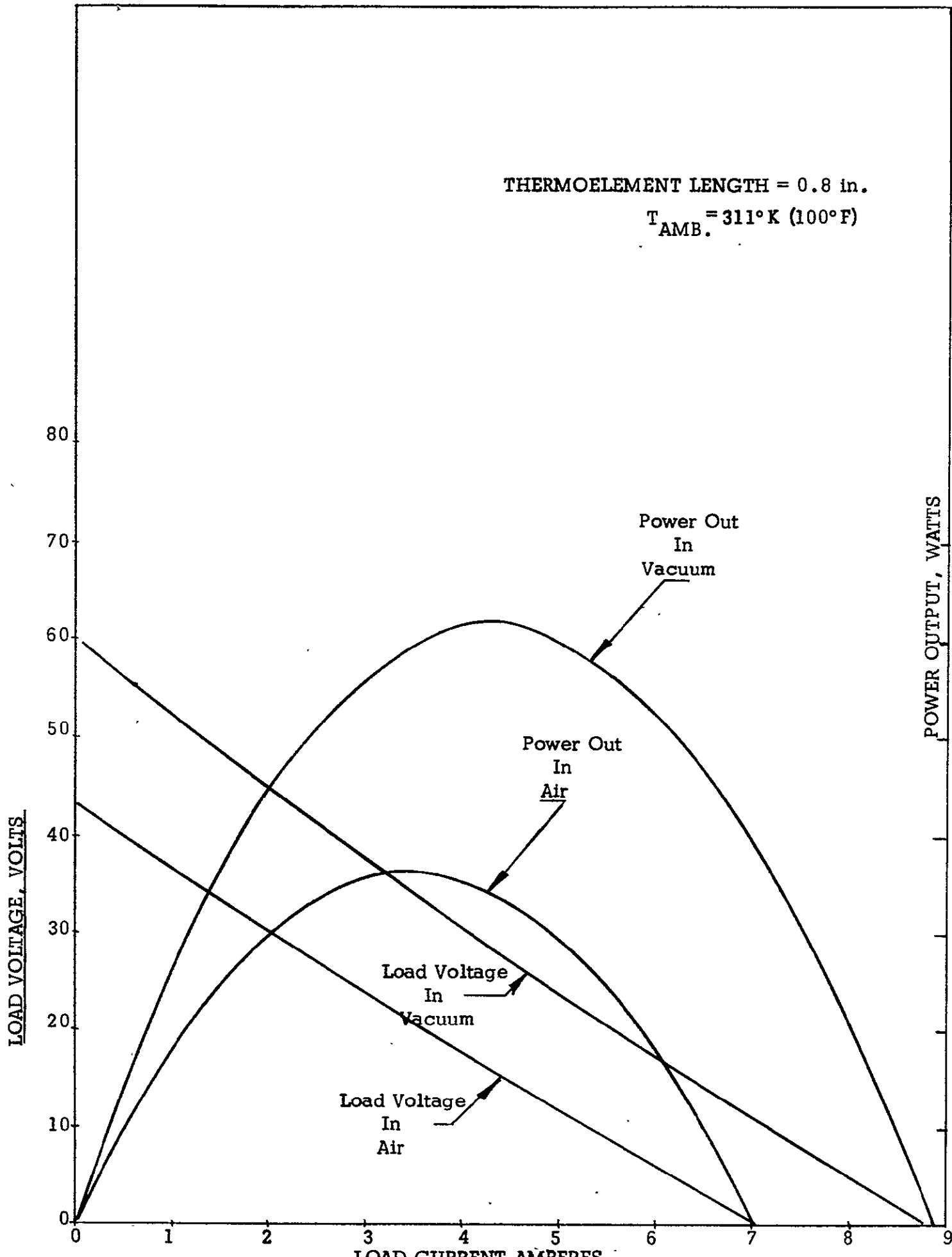

Fig. 15 Zr O_2 Insulated MHW - Generator Performance in Vacuum and Air

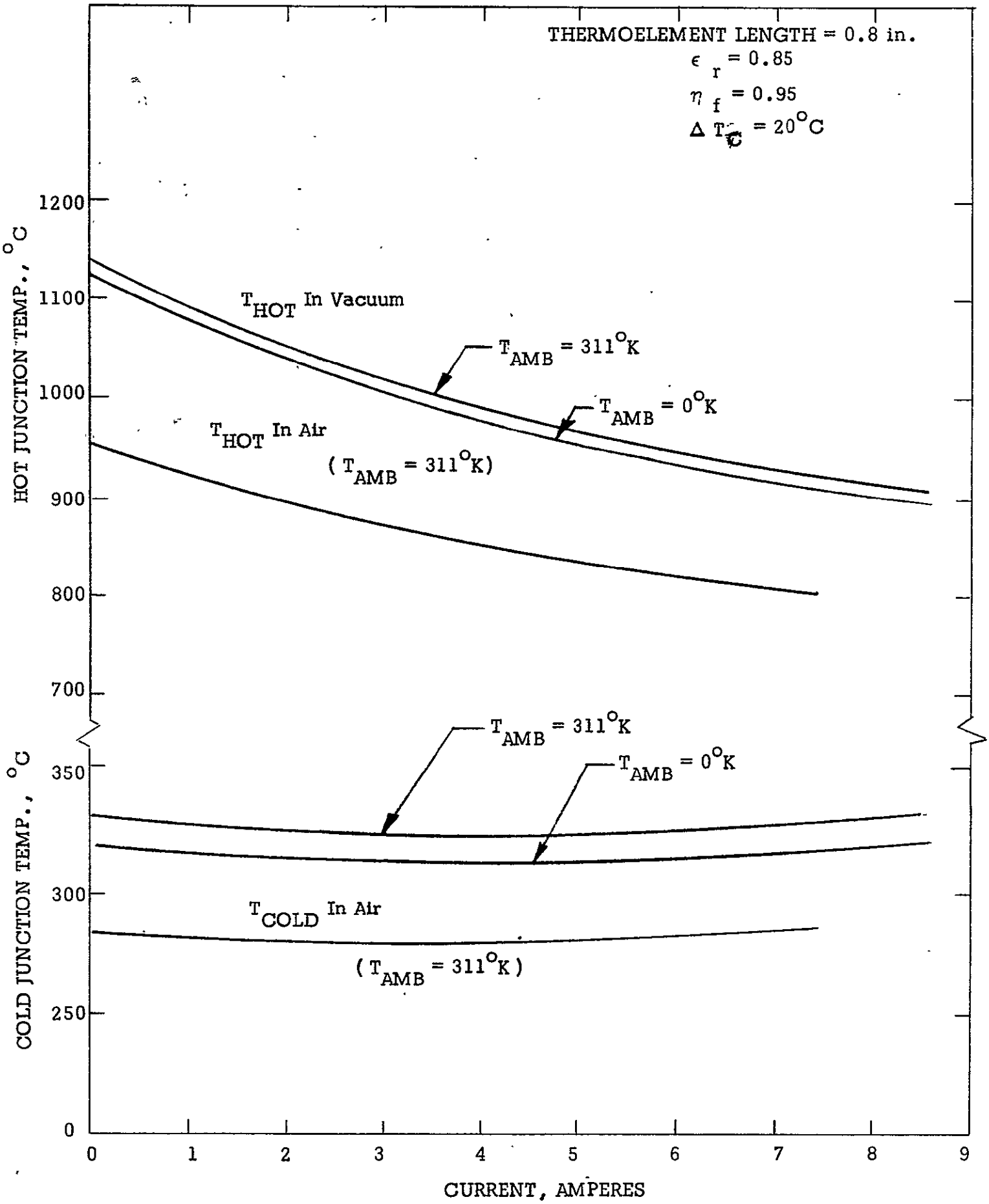

Fig.16 MIN-K 2020 Insulated MHW Generator Temperatures in Vacuum and Air

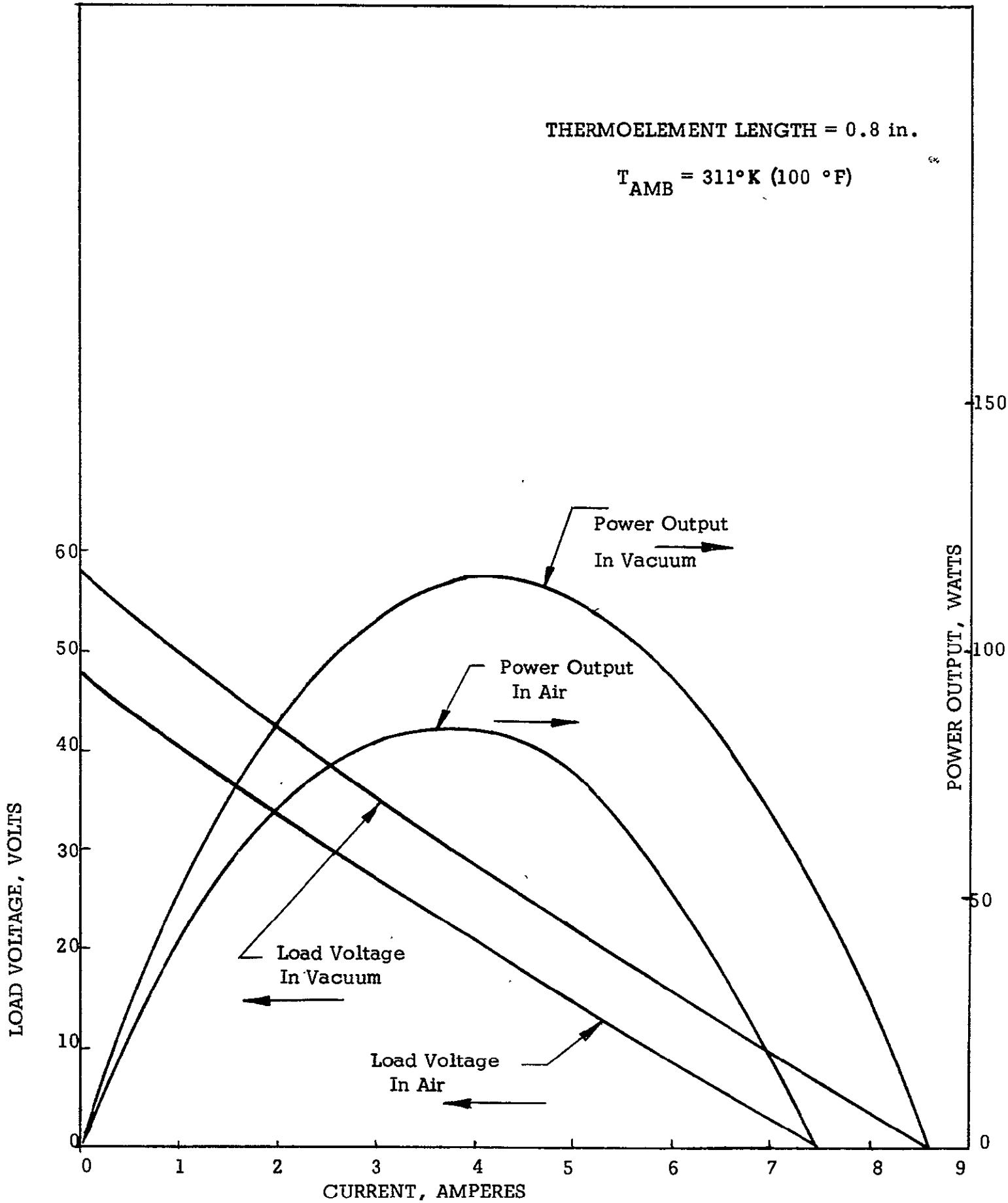

Fig. 17 Min-K 2020 Insulated MHW - Generator Performance in Vacuum and Air

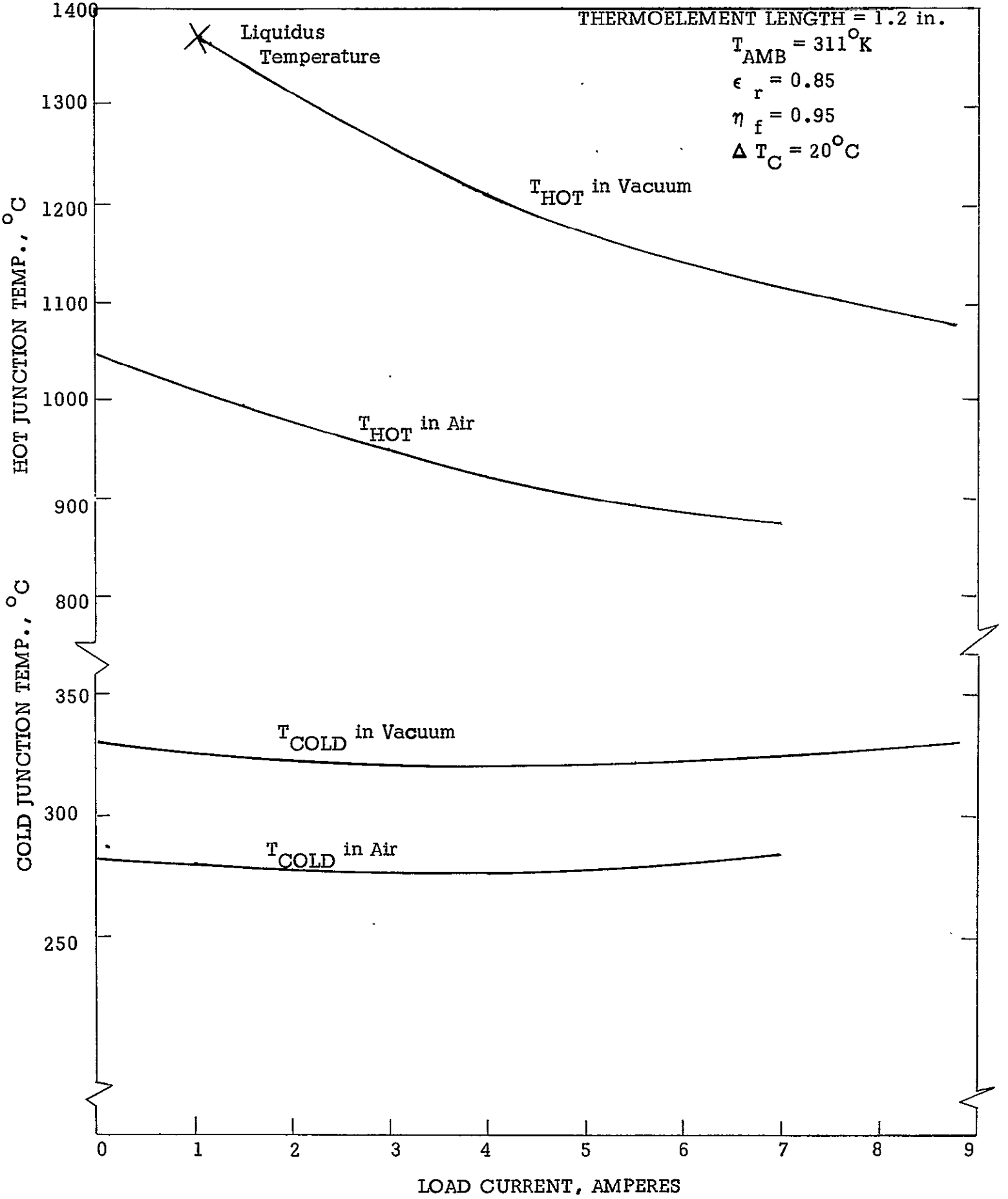

Fig. 18 Calculated MHW Generator Temp. - Foil Insulation

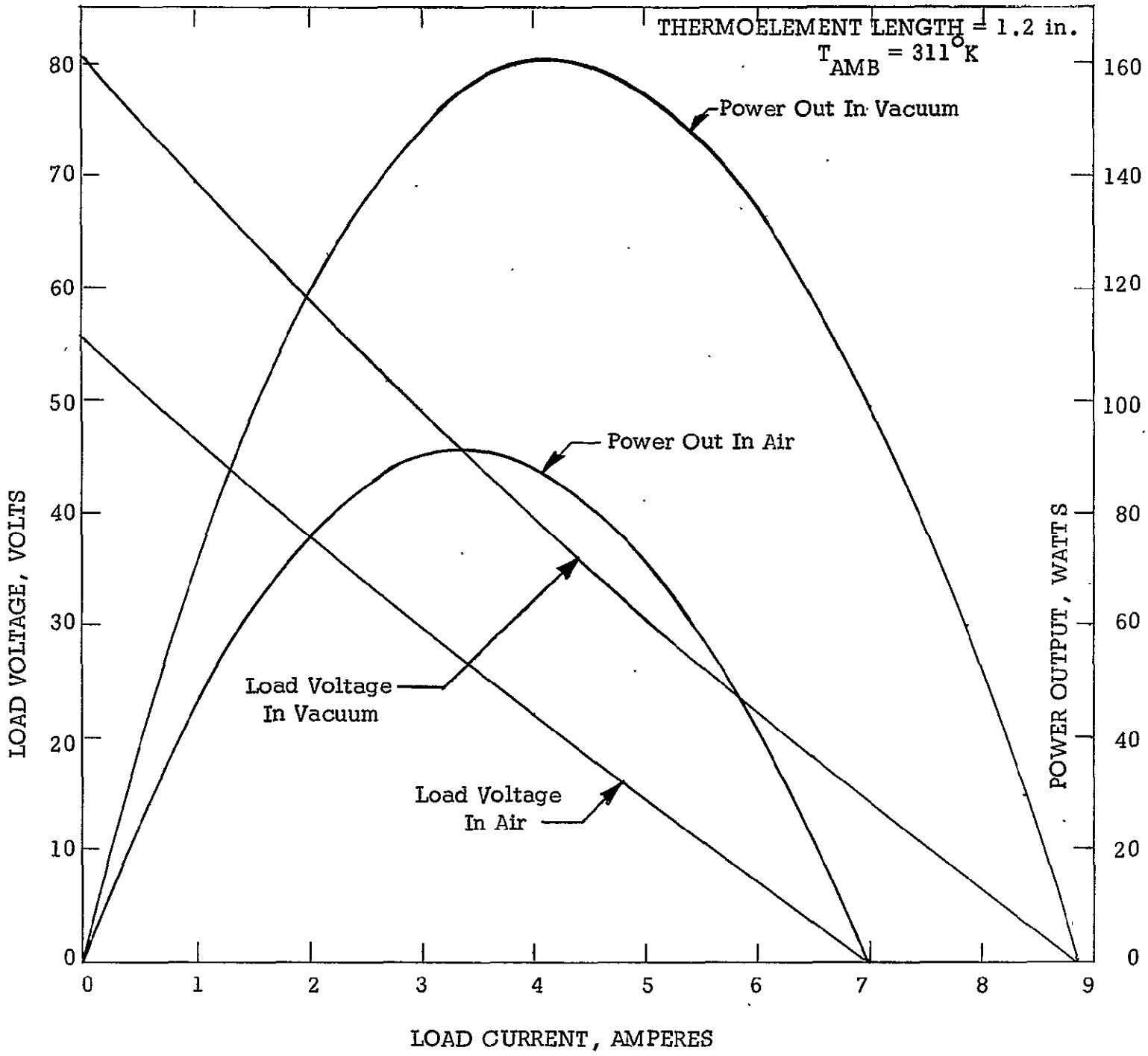

Fig. 19 Calculated MHW Generator Performance - Foil Insulation

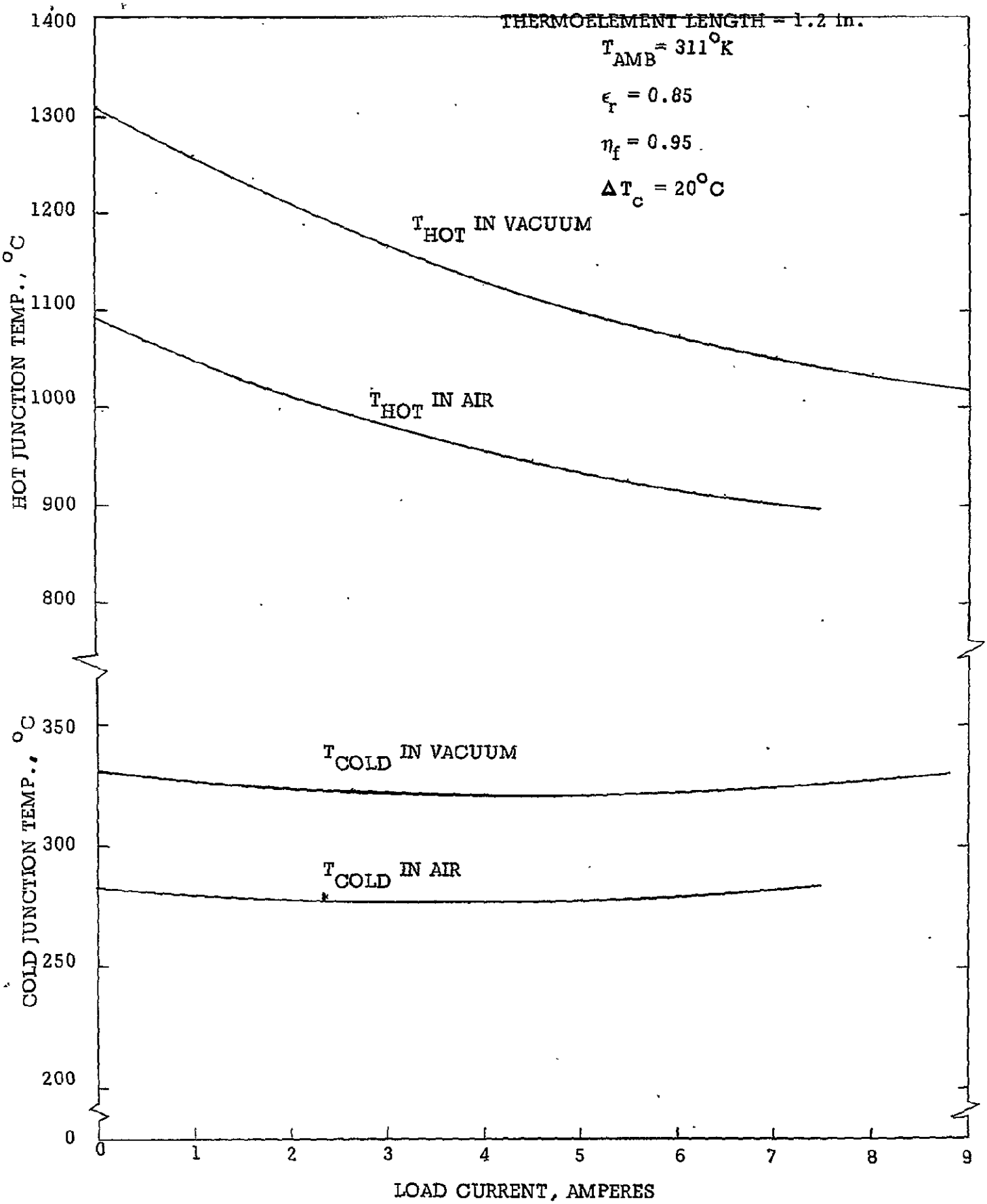

Fig. 20 CALCULATED MHW GENERATOR TEMP. - Zr 0_2 INSULATION

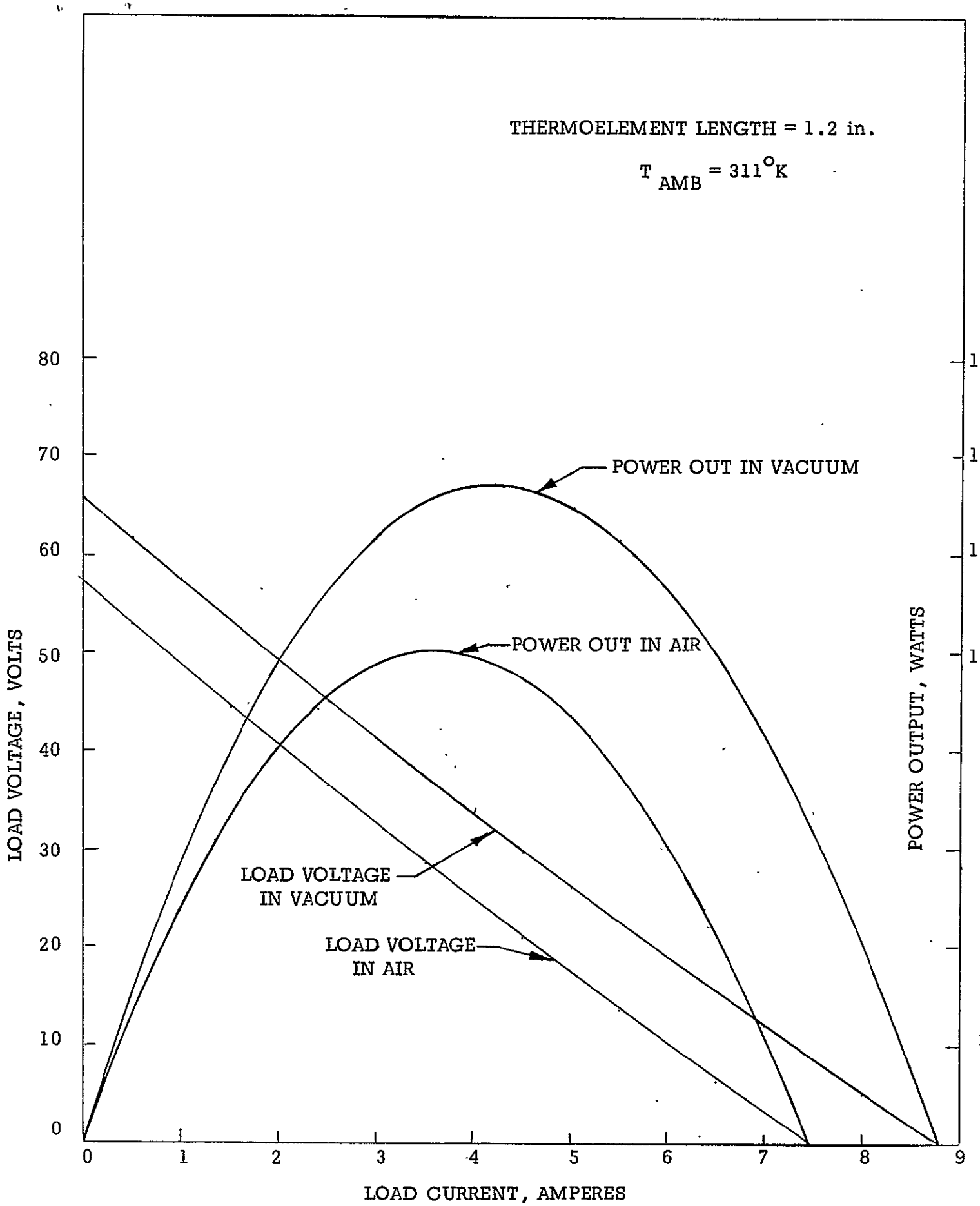

Fig. 21 CALCULATED MHW GENERATOR PERFORMANCE - $Zr\,0_2$ INSULATION

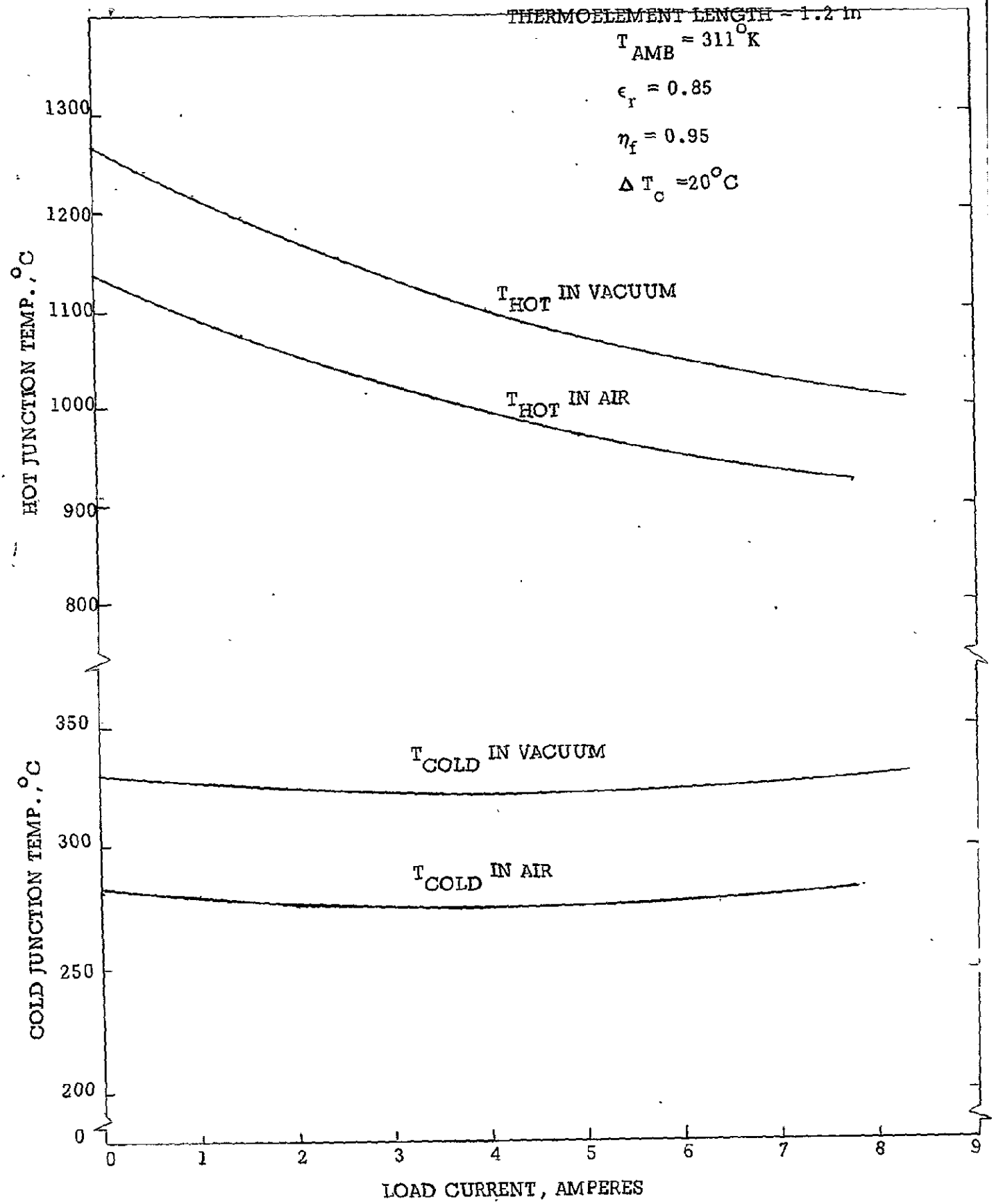

Fig.22 CALCULATED MHW GENERATOR TEMP. MIN - K 2020 INSULATION

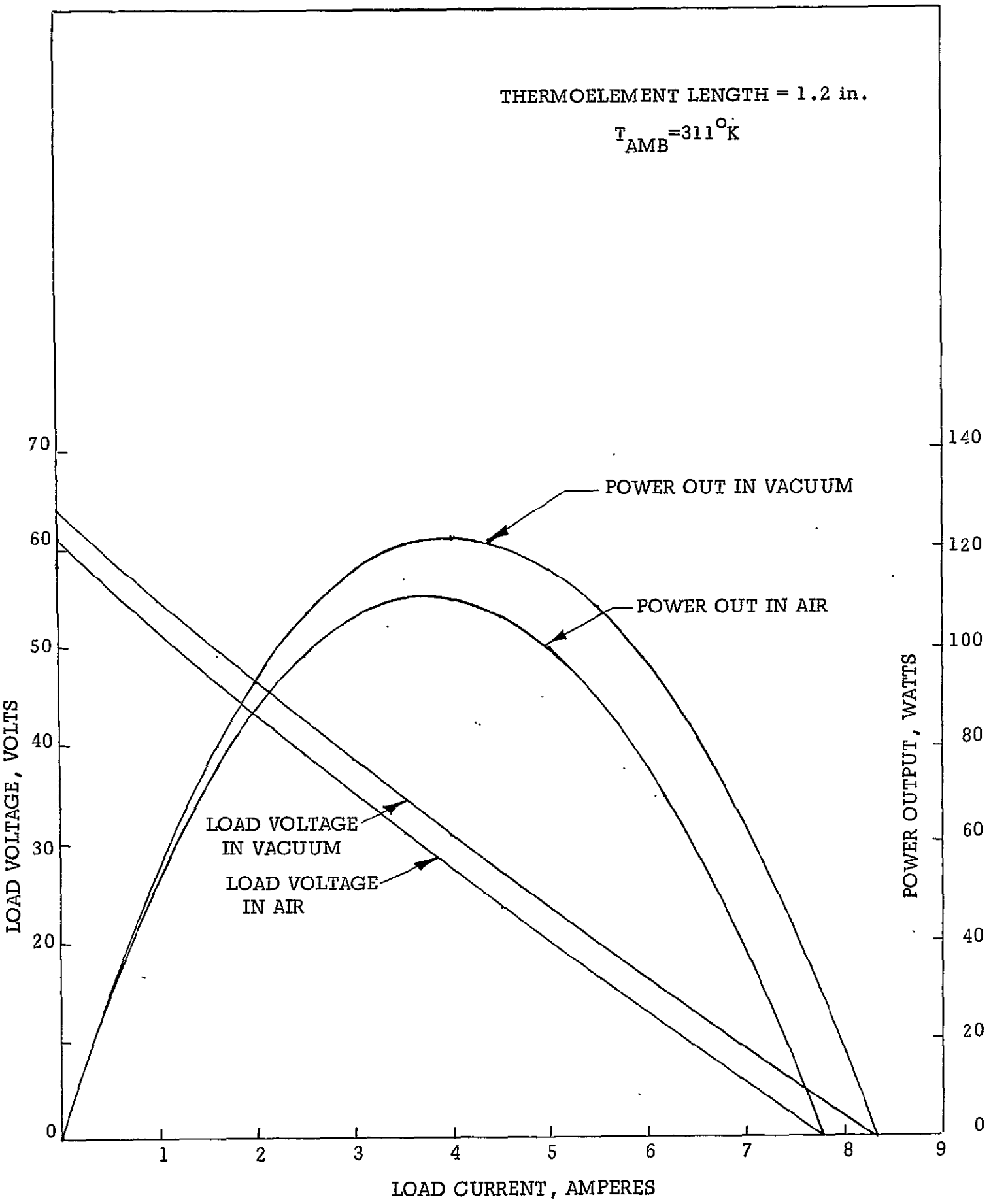

Fig. 23 CALCULATED MHW GENERATOR PERFORMANCE MIN - K 2020 INSULATION

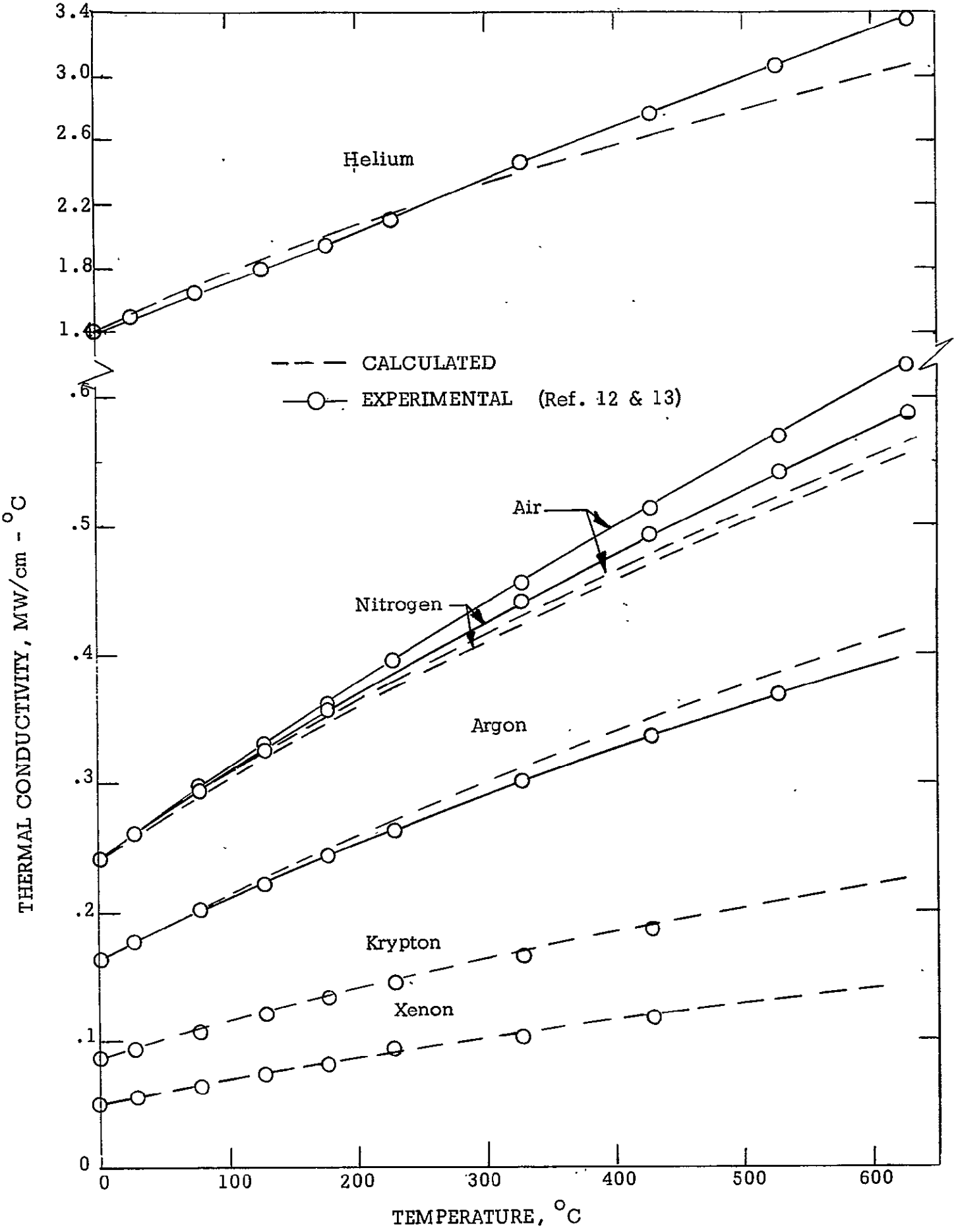

Fig.24 Thermal Conductivity of Gases

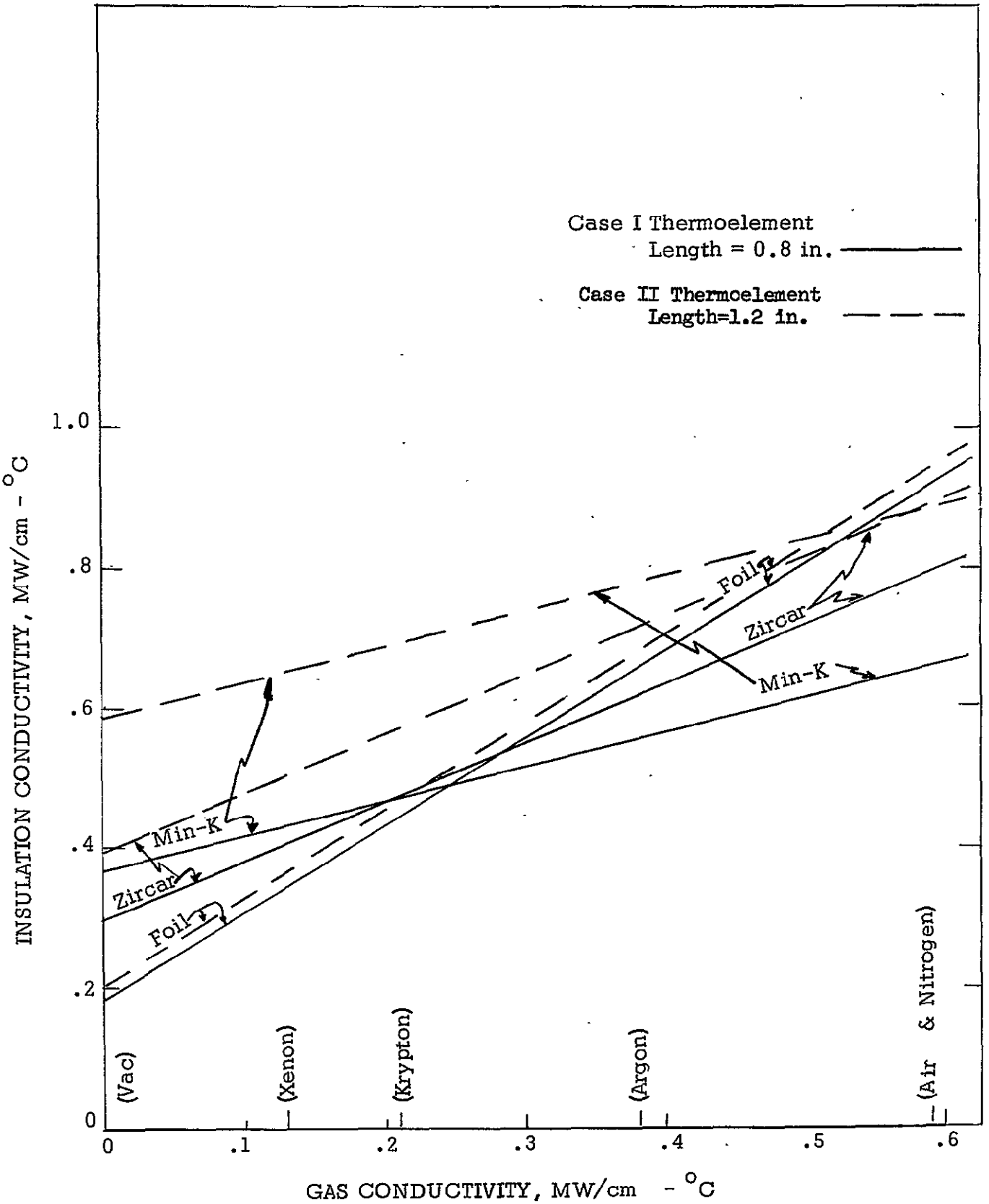

Fig.25 Effect of Gas on Insulation Conductivity corresponding to average Temperature of the thermoelement.

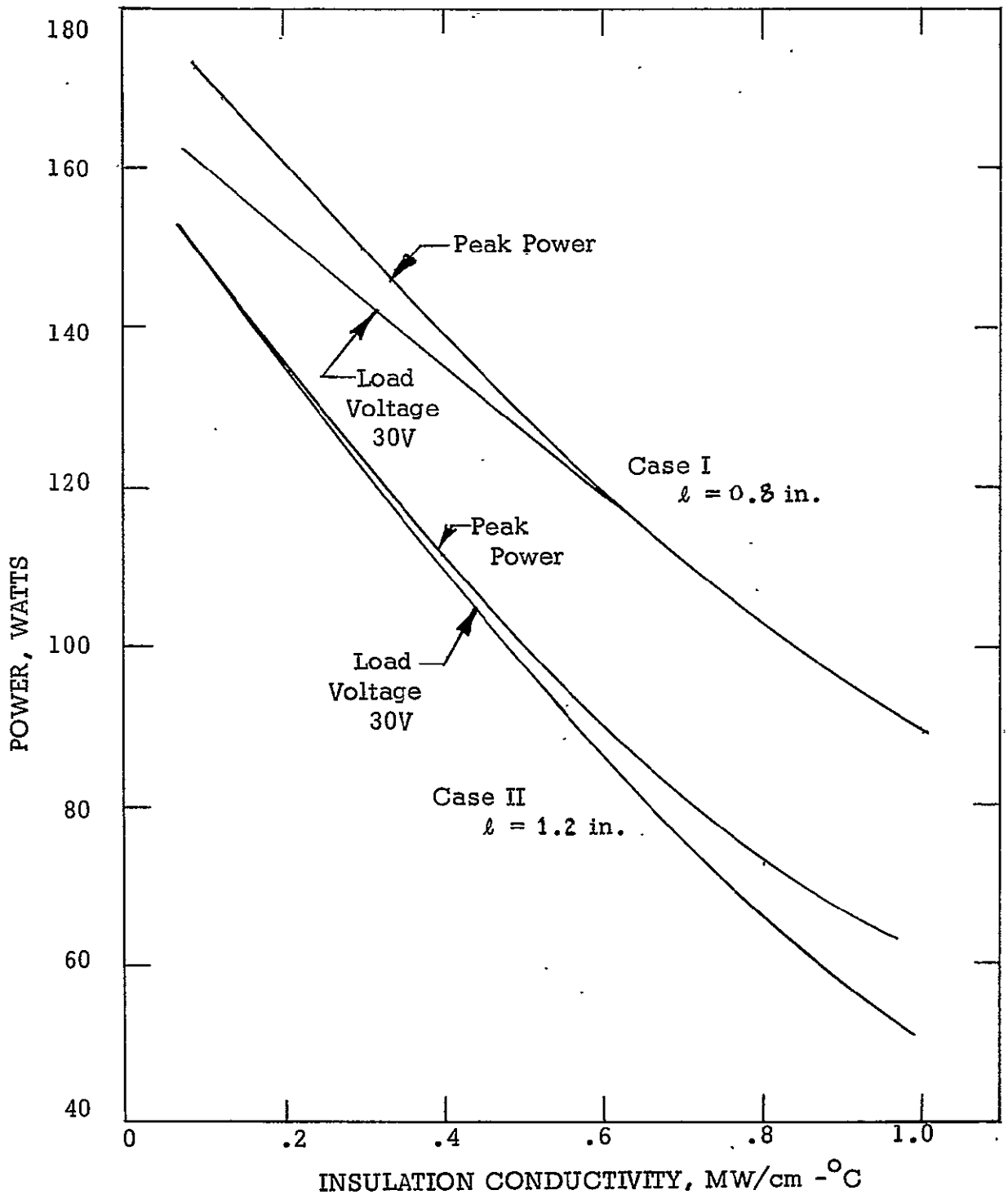

Fig.26 MHW-RTG Power Output

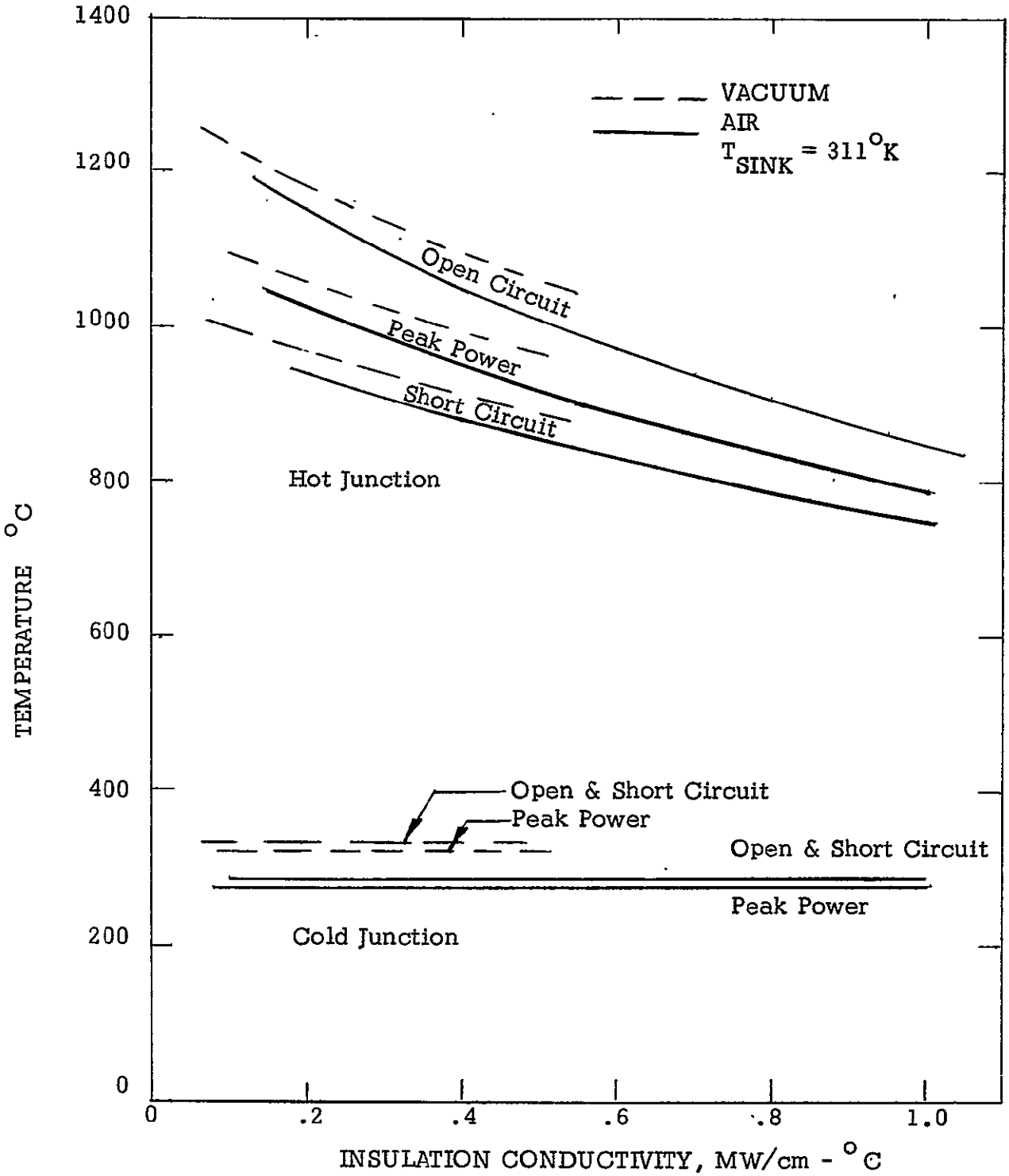

Fig.27 MHW-RTG Temperatures for Thermoelement Length = 0.8 in.

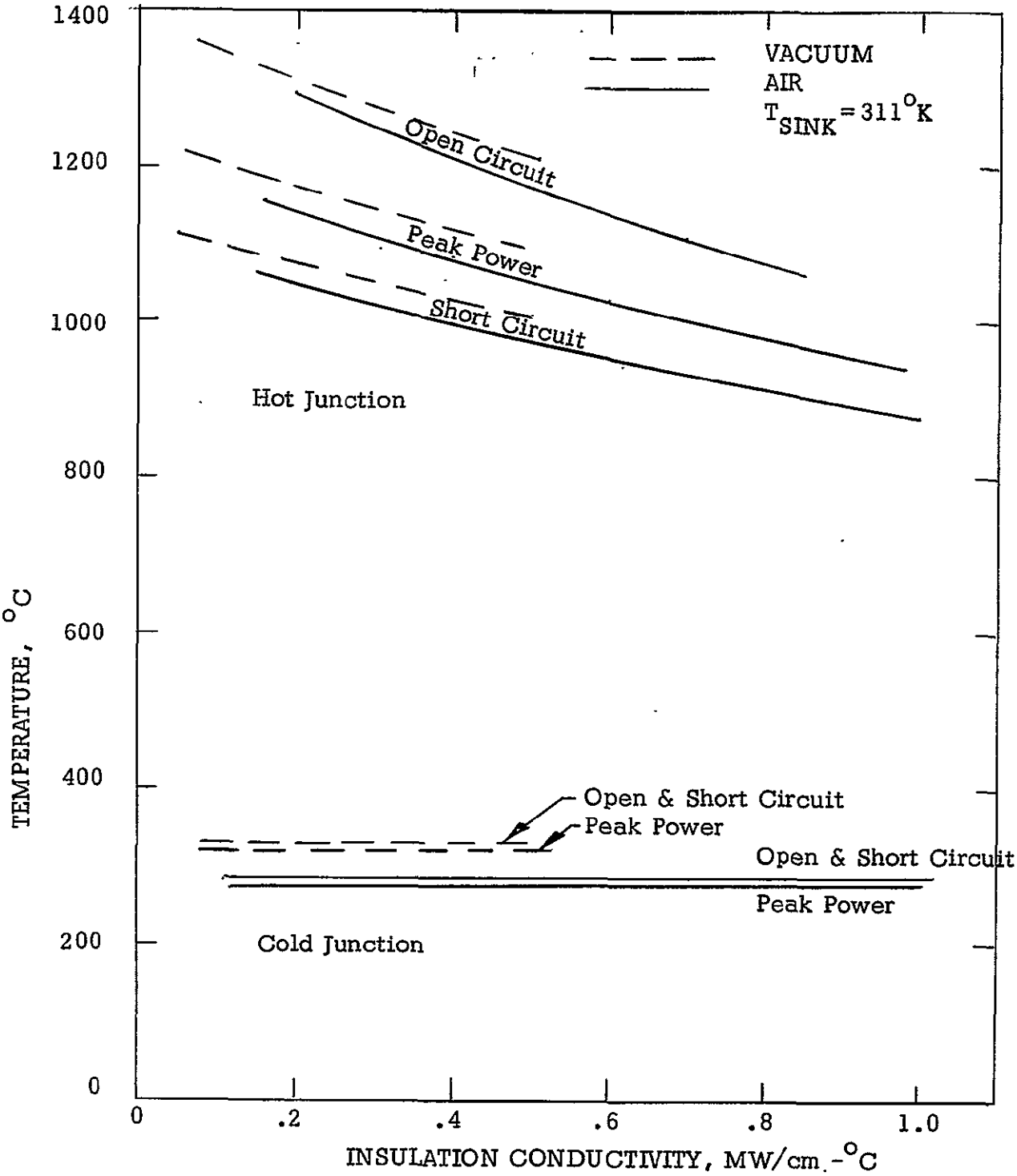

Fig. 28 MHW-RTG Temperatures for Thermoelement Length = 1.2 in.

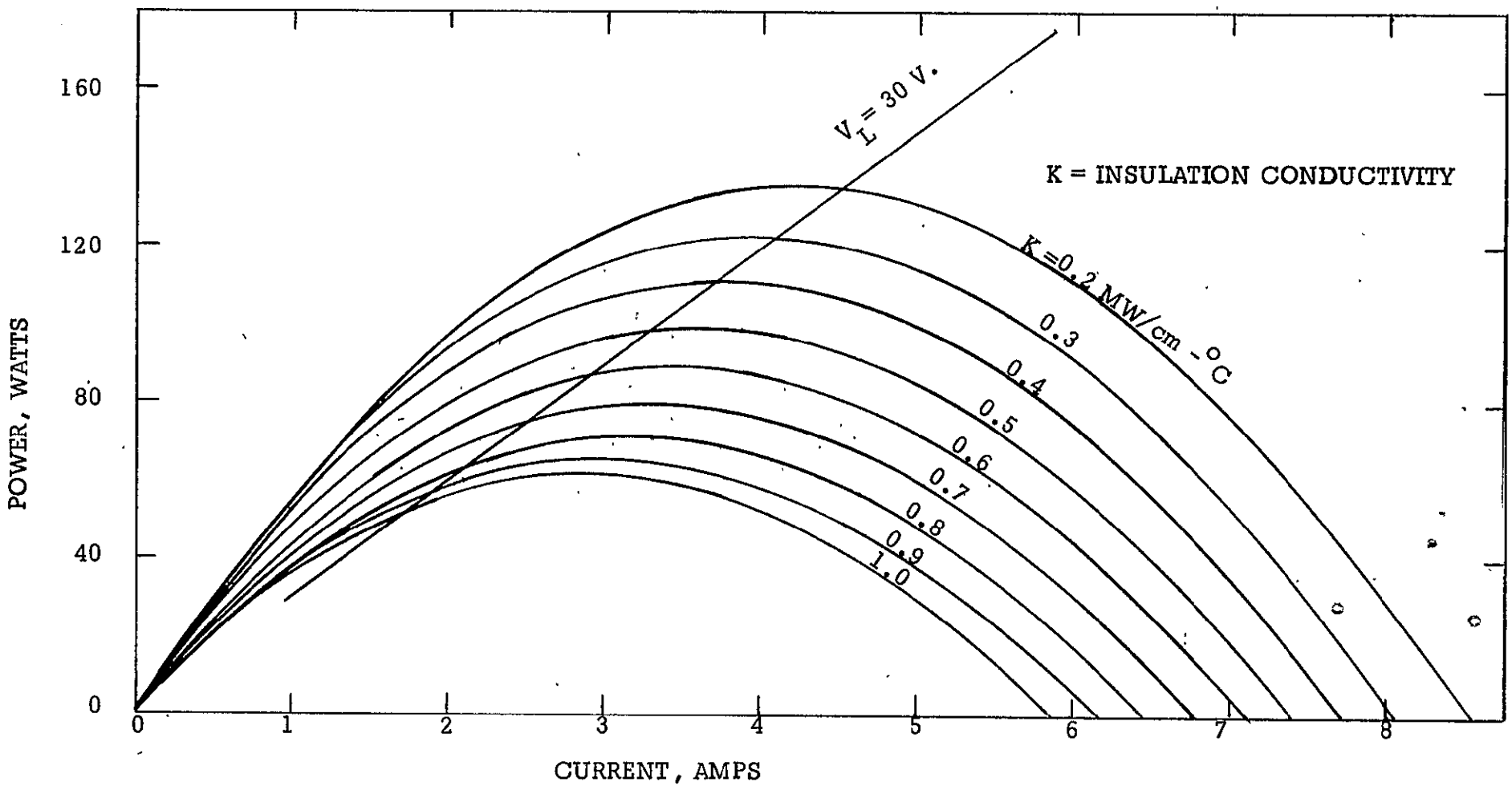

Fig.29 MHW-RTG Power Output for Thermoelement Length = 0.8 in.

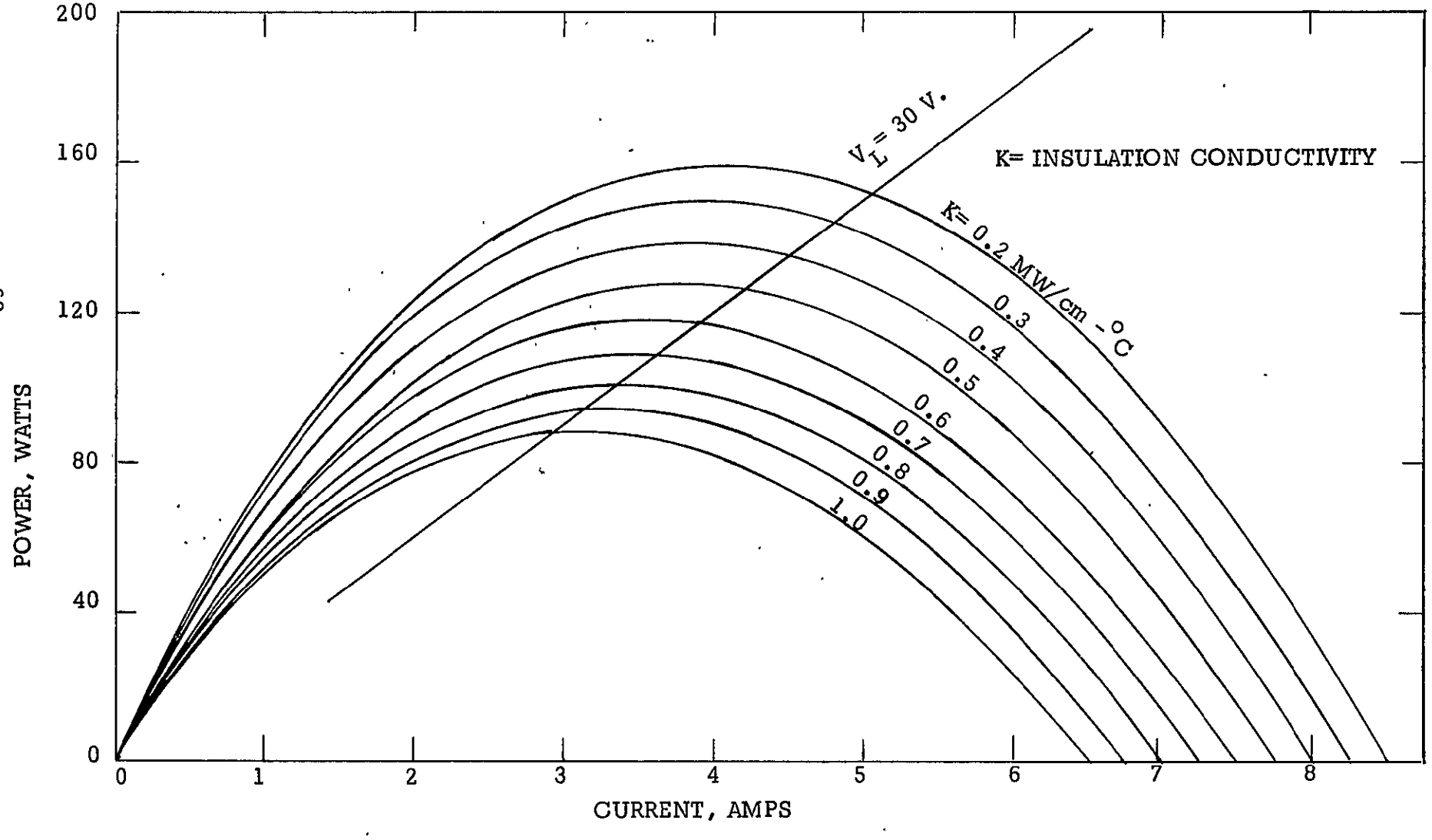

Fig. 30 MHW-RTG Power Output for Thermoelement Length = 1.2 in.

REFERENCES

1. V. Raag, "Optimization of Thermoelectric Generators for Fixed Temperature and Fixed Heat Input Operation", Memo #4 to JPL, Aug. 20, 1969.

2. A. F. Joffe, Semiconductor Thermoelements and Thermoelectric Cooling, Inosearch Limited, London, 1957.

3. R. L. Reid, "Air Exposure of Multifoil Insulation Systems", ASME Publication 68-HT-50, May 13, 1968.

4. M. Jakob, Elements of Heat Transfer, Chapt. VII, John Wiley & Sons, Inc., New York, 1954.

5. Johns-Manville Research and Engineering Center, Final Report, AEC Contract No. AT (29-2)-2661.

6. RCA, Twenty-Third Monthly Report on AEC Contract No. AT (29-2)-2510, Nov. 1969.

7. RCA, Twenty-Fourth Monthly Report on AEC Contract No. AT (29-2)-2510, Dec. 1969.

8. Private Communication, Richard Hemler, GE, Feb. 24, 1970.

9. V. Raag, "Thermoelectric Properties of 80 a/o Si - 20 a/o Ge Alloy as a Function of Time and Temperature", Memo #6 to JPL, March 3, 1970.

10. D. Leonard, I.O.M. to O. Merrill entitled "MHW-RTG Operation in Gas", dated April 28, 1970.

11. S. Chapman and T. Cowling, The Mathematical Theory of Non-Uniform Gases, Cambridge, 1960

12. J.R. Moszynski, Proceeding of the Fourth Symposium on Thermophysical Properties, ASME Publication, 1968, p. 323.

13. "Cryogenics & Industrial Gases", March, 1970.

14. "Elevated Temperature Thermal Conductivity Measurements of Fibrous Insulations", Fifth Conference on Thermal Conductivity, Denver, Colo. October 20, 1965, Vol. II.

APPENDIX A - AVERAGE THERMOPHYSICAL PROPERTIES

The temperature dependence of various thermophysical properties requires the definition of average values for the properties to be used algebraically in thermoelectric generator performance equations. By assuming no radiation losses and no internal heat source/heat sink, the average thermal conductivity, Seebeck coefficient and electrical resistivity may be defined as follows:

THERMAL CONDUCTIVITY

The heat conduction equation may be written as

$$q = \text{constant} = k(T)\,\frac{dT}{dx} = \langle k\rangle\,\frac{\Delta T}{\ell} \tag{A1}$$

Integration of Eq. (A1) and the use of appropriate limits of integration yields

$$\int_{T_C}^{T_H} k(T)\,dT = \int_{0}^{\ell} \langle k\rangle\,\frac{\Delta T}{\ell}\,dx = \langle k\rangle\,\frac{\Delta T}{\ell}\int_{0}^{\ell} dx = \langle k\rangle\,\Delta T \tag{A2}$$

Upon rewriting, the average thermal conductivity may be defined as

$$\langle k\rangle = \frac{1}{\Delta T}\int_{T_C}^{T_H} k(T)\,dT \tag{A3}$$

SEEBECK COEFFICIENT

The averaged Seebeck coefficient is obtained from its definition by integration

$$V = \int_{T_C}^{T_H} S(T)\,dT = \int_{T_C}^{T_H} \langle S\rangle\,dT = \langle S\rangle\int_{T_C}^{T_H} dT = \langle S\rangle\,\Delta T \tag{A4}$$

Upon rewriting, the average Seebeck Coefficient may be defined as

$$\langle S\rangle = \frac{1}{\Delta T}\int S(T)\,dT \tag{A5}$$

ELECTRICAL RESISTIVITY

The definition of average electrical resistivity requires the inclusion of a non-linear temperature profile. The average electrical resistivity is defined by

$$\langle\rho\rangle \frac{\ell}{A} = \frac{1}{A}\int_0^{\ell} \rho\,(T\ (x)\ )\,dx \tag{A6}$$

Solution of Eq. (A1) for the differential dx, the substitution of this into Eq. (A6) and rearrangement yields

$$\langle\rho\rangle = \frac{1}{\ell}\int_{T_C}^{T_H} \rho\ (T)\ \frac{k(T)}{q}\ dT \tag{A7}$$

The substitution of Eqs. (A1) and (A3) into Eq. (A7) finally gives

$$\langle\rho\rangle = \frac{\int_{T_C}^{T_H} \rho\,(T)\,k(T)\,dT}{\int_{T_C}^{T_H} k(T)\,dT} \tag{A8}$$

Equations (A3), (A5), and (A8) serve to define the average thermophysical properties of the thermoelements. Providing the temperature limits of integration are known, the averaged properties are constant numeric values which may be used algebraically in the performance equations.

APPENDIX B - COMPUTER PROGRAM

The computer program reproduced in this Appendix was used to perform all of the calculations reported in the present memorandum. The program is written in BASIC language and in its entirety is used to calculate generator performance in either vacuum or air. To calculate generator performance in vacuum operation, the convective coefficient, K_4, is set equal to zero. The effect of gases upon the thermal insulation is reflected in the value calculated for K4. The instruction GOSUB 720 (line 690) is an output format sub-routine. The following definition of symbols applies to the computer program.

Input

$Q1 = Q_{in}$	=	total heat input, watts
$E1 = \epsilon_r \eta_f F$	=	combined effective emissivity, fin effect and view factor
$A1 = A_R$	=	radiative area, cm^2
$A5 = A_c$	=	convective area, cm^2
$K2 = \langle k_p \rangle$	=	averaged p-type thermoelement thermal conductivity, watt/cm° K
$K3 = \langle k_n \rangle$	=	averaged n-type thermoelement thermal conductivity, watt/cm° K
$A2 = a_p$	=	p-type thermoelement area, cm^2
$A3 = a_n$	=	n-type thermoelement area, cm^2
$N = N$	=	total number of couples
$A4 = A_e$	=	effective insulation area, cm^2
$K4 = \langle k_I \rangle$	=	effective insulation thermal conductivity, watt/cm° K
$L = \ell$	=	thermocouple length, cm
$R2 = \rho_p$	=	p-type thermoelement electrical resistivity, Ω-cm
$R3 = \rho_n$	=	n-type thermoelement electrical resistivity, Ω-cm
$S = \lvert\langle S_n \rangle\rvert + \lvert\langle S_p \rangle\rvert$	=	combined n-and p-type thermoelement Seebeck coefficient, v/° K
$R4 = \delta$	=	electrical loss factor

$N1 = N_S$	=	number of thermocouples in series
$N2 = n$	=	number of parallel electrical branches
$Y = \Delta T_C$	=	cold-stack temperature drop
$K5 = K$	=	convective heat transfer coefficient

Output

$M = m$	=	R_L/R_g
$T1 = T_C$	=	cold junction temperature, °C
$T2 = T_H$	=	hot junction temperature, °C
$V = V_L$	=	load voltage, volts
$P = P_o$	=	power output, watts
$E = \eta$	=	efficiency, percent
$I = I$	=	load current, amps

```
GET-GEN
LIST
GEN

10  REM Q1=HEAT INPUT,E1=EFF. EMISSIVITY,A1=RADIATIVE AREA
20  REM A5=CONVECTIVE AREA, K2=THERM. COND OF P-LEG
30  REM K3=THERM. COND OF N-LEG, A2=AREA OF P-LEG
40  REM A3=AREA OF N-LEG, N=# OF COUPLES,A4=AREA OF INSULATION(EFF.)
50  REM K4= INS. EFF. COND.,L=COUPLE LENGTH,R2=P-LEG RES.
60  REM R3= N-LEG RES.,S=SEEBECK COEFF, R4=ELECT. LOSS,N1=#SERIES COUP.
70  REM N2= # PARALLEL BRANCHES, Y= DELTA TC, K5=CONVECTIVE COEFF.
80  PRINT "ENTER VALUES FOR Q1,E1,A1,A5,K2,K3,A2,A3,N"
90  INPUT Q1,E1,A1,A5,K2,K3,A2,A3,N
100  PRINT "ENTER VALUES FOR A4,K4,L,R2,R3,S,R4,N1,N2,Y,K5"
110  INPUT A4,K4,L,R2,R3,S,R4,N1,N2,Y,K5
120  FOR I=1 TO 4
130  PRINT
140  NEXT I
150  PRINT "PROGRAM TO CALCULATE T/E GENERATOR PERFORMANCE"
160  PRINT TAB(15);"HEAT INPUT=";Q1
170  PRINT
180  PRINT
190  PRINT " M       TC     TH     VL      PO      EFF     I"
200  PRINT
210  REM
220  FOR M=0 TO 2 STEP .2
230  GOSUB 320
240  NEXT M
250  FOR M=3 TO 10 STEP 1
260  GOSUB 320
270  NEXT M
280  FOR M=15 TO 60 STEP 5
290  GOSUB 320
300  NEXT M
310  END
320  Q2=.95*Q1
330  A=5.67E-12*E1*A1
340  F3=A5*K5
350  LET F=6
360  X=0
370  T=A↑(-.25)*(.975*(1-E/100)*Q1)↑.25
380  X=X+1
390  F1=A*(T↑4-311↑4)+F3*(T-311)↑1.25-(1-E/100)*.975*Q1
400  F2=4*A*T↑3+1.25*F3*(T-311)↑.25
410  T=T-F1/F2
420  IF ABS(F1/F2)<.1 THEN 440
430  GOTO 390
440  REM
450  C=T+Y
460  T1=C-273
470  K=(K2*N*A2+K3*N*A3)*1/L+K4*(A4-N*A2-N*A3)*1/L
480  R1=(R2/A2+R3/A3)*L
490  G=(N*S↑2)/(2*K4*R1*(1+M)↑2)
500  B=(2*M*C-K/G)*1/(1+2*M)
510  D=(C2/G+(K/G)*C+C↑2)*1/(1+2*M)
520  H=(B+(B↑2+4*D)↑.5)*1/2
530  T2=H-273
540  D1=H-C
```

```
550  V=(M/(1+M))*N1*S*D1
560  R5=(N1/N2)*R4*R1
570  P=(M/(1+M))↑2)*(N1*S*D1)↑2*1/R5
580  E=P/Q1*100
590  IF X<4 THEN 380
600  I=(1/(1+M))*N1*S*D1*1/R5
610  Z[1]=M
620  Z[2]=T1
630  Z[3]=T2
640  Z[4]=V
650  Z[5]=P
660  Z[6]=E
670  Z[7]=I
680  Z$="##.#  ####  ####  ##.##  ###.##  ##.##  ##.##"
690  GØSUB 720
700  RETURN
710  STØP
720  REM  *****  FØRMAT  *****  UTILITY SUBRØUTINE  *****
730  REM  *****  VERSIØN 1  *****  7/31/69  *****
740  REM  SUBRØUTINE TØ FØRMAT A PRØGRAM'S DATA
750  LET Z2=Z3=Z4=Z5=Z7=Z8=Z9=1
760  DIM Y$[10],Z$[72]
770  LET Y$="0123456789"
780  LET ZØ=Z9-1
790  LET ZØ=ZØ+1
800  IF ZØ=LEN(Z$)+1 THEN 1310
810  IF Z$[ZØ,ZØ]="#" THEN 880
820  IF Z$[ZØ,ZØ+1]=".#" THEN 880
830  IF Z$[ZØ,ZØ+1]="+#" THEN 860
840  PRINT Z$[ZØ,ZØ];
850  GØTØ 790
860  LET Z4=0
870  GØTØ 790
880  LET Z=100
890  LET Z6=Z[Z2]
900  LET Z9=ZØ-1
910  LET Z9=Z9+1
920  IF Z$[Z9,Z9]="." THEN 950
930  IF Z$[Z9,Z9]="#" THEN 910
940  GØTØ 990
950  IF Z5#1 THEN 990
960  LET Z5=0
970  LET Z=Z9
980  GØTØ 910
990  IF Z#100 THEN 1010
1000  LET Z=Z9
1010  IF Z4=1 THEN 1060
1020  IF Z6 >= Ø THEN 1050
1030  PRINT "-";
1040  GØTØ 1060
1050  PRINT " ";
1060  LET Z6=ABS(Z6)+10↑(Z-Z9-1)
1070  FØR Z1=Z-ZØ TØ Z+1-Z9 STEP -1
1080  IF Z$[Z-Z1,Z-Z1]#"." THEN 1130
1090  PRINT ".";
1100  LET Z3=0
```